UNMANNED AERIAL VEHICLE (UAV) DATASETS FOR RETRIEVAL OF FOREST PARAMETERS AND ESTIMATION OF ABOVEGROUND BIOMASS IN BERKELAH TROPICAL RAINFOREST, MALAYSIA

BELINDA ENUWAMHANGBE ODIA
February, 2018

SUPERVISORS:
Ir L.M. van Leeuwen – de- Leeuw
Dr. Y.A. Hussin

ADVISOR:
Dr. Zulkiflee Abd Latif

UNMANNED AERIAL VEHICLE (UAV) DATASETS FOR RETRIEVAL OF FOREST PARAMETERS AND ESTIMATION OF ABOVEGROUND BIOMASS IN BERKELAH TROPICAL RAINFOREST, MALAYSIA

BELINDA ENUWAMHANGBE ODIA
Enschede, The Netherlands, February, 2018

Thesis submitted to the Faculty of Geo-Information Science and Earth Observation of the University of Twente in partial fulfilment of the requirements for the degree of Master of Science in Geo-information Science and Earth Observation.
Specialization: Natural Resource Management

SUPERVISORS:
Ir L.M. van Leeuwen – de- Leeuw
Dr. Y.A. Hussin

ADVISOR:
Dr. Zulkiflee Abd Latif

THESIS ASSESSMENT BOARD:
Prof. Dr. A.D. Nelson (Chair)
Dr. T. Kauranne (External Examiner, Lappeenranta University of Technology, Finland)

ABSTRACT

Conventional method of estimating Aboveground biomass (AGB) are based on field measurements and destructive sampling technique, however, this methods are time-consuming, labour intensive and unsustainable. Remote sensing technology offers a non-destructive method for the estimation of aboveground biomass through allometric equations that require forest parameters such as tree height, Diameter at Breast Height (DBH) and/or crown projection area (CPA). The use of Unmanned Aerial Vehicle (UAV) derived data surpassed the limitations of other remote sensing methods that has been done to retrieve these forest parameters. In this study, we evaluated the retrieval of forest biophysical parameters from UAV data across three study sites in a tropical forest ecosystem. Canopy Height Model was generated exclusively from UAV data for the estimation of forest tree height and in comparison to forest tree height estimated from airborne LiDAR data. Comparison of the retrieved forest height was based on regression and the root mean square error method. Furthermore, Object Based Image analysis (OBIA) was used to extract individual tree crown projection area from the orthophoto. The resultant CPA was used to establish relationship with DBH. Afterwards, to assess the effect of predicted DBH, AGB was estimated and compared between using ground truth and predicted DBH in combination with forest tree height derived from UAV CHM. The results of the tree height comparison revealed overestimation by the airborne LiDAR due to errors in the DTM. The validation of the tree segmentation was equally good and a positive significant relationship was found between CPA and field sampled DBH. There was no significant difference between using predicted and field measured DBH for the estimation of AGB. In conclusion, the use of 3D photogrammetry of images acquired using UAV offers a reliable data source for extraction of forest biophysical parameters to assess AGB in tropical rainforests.

Keywords: Aboveground biomass, Allometric equation, tree height, DBH, CPA, UAV, CHM, airborne LiDAR, orthophoto.

ACKNOWLEDGEMENTS

My appreciation goes to the Almighty God for his protection and granting me good health from the commencement and completion of my study.

My profound gratitude goes out to my first supervisor, Ir. L.M. van Leeuwen – de – Leeuw for her patience, encouragement, and advice from the beginning to the completion of this thesis. My appreciation goes to my second supervisor, Dr. Yousif A. Hussin for his feedback, continuous encouragement and advice My sincere thanks to Prof. Dr. A.D. Nelson for his constructive criticism and feedback during the proposal defence and mid-term review presentations.

I want to also use this medium to appreciate Dr Zulkiflee Abd Latif and Ms Syaza Rozali of the MARA Univerisity of Malaysia (UiTM), for their hospitality and support throughout the fieldwork period.

I will be ungrateful if I fail to acknowledge my friends; Agbor Esong Efiong, Okojie Jefferson, Musa Ahmed, Akejiori Ilamosi Juliet and Robert Masolele who made my stay at ITC interesting and helped me overcame challenges I faced during the course of this study.

I am grateful to the Netherlands Fellowship Programme (NFP) for granting me a scholarship to pursue my Masters at ITC, University of Twente, and my employer; the National Space Research and Development Agency (NASRDA) for granting me a leave to study at the Netherlands.

I am highly indebted to my parents for their sacrifice, spiritual and moral support. Their prayers and encouragemnt served as a fuel to help me complete this study. To my siblings, I am grateful for your love and patience during my long absence. Finally, to the entire NRM class of the 2016-2018 session, it was a pleasure spending this 18 months together as one big family.

Belinda Enuwamhangbe Odia
February, 2018
Enschede, The Netherlands.

TABLE OF CONTENTS

LIST OF FIGURES

LIST OF TABLES

LIST OF EQUATIONS

LIST OF ACRONYMS

AGB	Aboveground biomass
ALS	Airborne Laser Scanner
ANOVA	Analysis of variance
CHM	Canopy Height Model
CO2	Carbon dioxide
CPA	Crown projection area
DBH	Diameter at Breast Height
DEM	Digital Elevation Model
DGPS	Differential Global Positioning System
DSM	Digital Surface Model
DTM	Digital Terrain Model
GCP	Ground control points
GNSS	Global Navigation Satellite System
GPS	Global Positioning System
IMU	Inertial Measurement Unit
InSAR	Interferometric Synthetic Aperture Radar
LiDAR	Light Detection and Ranging
MRVs	Monitoring Reporting and Verifications
OBIA	Object-Based Image Analysis
RADAR	Radio Detection and Ranging
REDD+	Reducing Emissions from Deforestation and Forest Degradation
RMSE	Root Mean Square Error
RPA	Remotely Piloted Aircraft
SFM	Structure From Motion
TLS	Terrestrial Laser Scanner
UAV	Unmanned Aerial Vehicle

1. INTRODUCTION

1.1. Background

Climate change is instigated by an increase in the amount of greenhouses gases, precisely the release of carbon dioxide (CO2) to the atmosphere (Grace, Mitchard, & Gloor, 2014). Fossil fuels and land use change are the leading anthropogenic causes of carbon dioxide emission into the atmosphere (Houghton et al., 2012; Malhi, 2010).

Forests cover 31 percent of the total land area of the globe. Tropical rainforests play a significant role in climate change mitigation because of their unique storage and sequestration of carbon (Gibbs, Brown, Niles, & Foley, 2007). On the other hand, in the tropics, forest degradation and deforestation is the main threat to the terrestrial carbon sinks and the balance of atmospheric greenhouse gases (Goetz et al., 2015; Malhi, 2010).

Tree biomass including undergrowth vegetation, dead wood and soil organic carbon constitutes the biomass within the forest ecosystems. Approximately 50% of dry forest biomass contains carbon (Zaki, Latif, Suratman, & Zainal, 2016). Estimating forest biomass is used to determine carbon sequestration rates and understanding the consequences of human actions on the terrestrial carbon cycle (Cao et al., 2016). Also, estimation of forest biomass gives an indication of the amount of carbon stock that has been sequestered in the forests or emitted to the atmosphere.

The role of tropical rainforests to combat climate change has been given attention by the United Nations Framework Convention on Climate Change (UNFCCC), by the introduction of Reducing Emissions from Deforestation and Forest Degradation (REDD+) programme. The REDD+ programme provide incentives to developing countries to reduce emissions from forested land. Within the REDD+ framework, Monitoring Reporting and Verification (MRV) is a mechanism used to ensure accurate estimation of carbon. Whereby, incentives are paid after quantified, reported and verifiable reduced emission levels.

Above ground biomass is the total quantity of aboveground oven-dry mass of a tree expressed in tons per unit area (Dubayah et al., 2010). Conventional method of estimating AGB is based on field measurements and destructive sampling technique. However, this methods are time-consuming, labour intensive and unsustainable (Kankare et al., 2013). Also, using these methods, it would not be possible to sample large area and access remote areas. Furthermore, monitoring and evaluation of carbon fluxes would not be possible with the traditional method.

On the other hand, remote sensing technology is a non-destructive method for the estimation of biomass. It allows repetitive coverage, and can access remote areas. In this regard, the use of remote sensing based approaches for estimation of biomass has gained recognition in the scientific domain. A non-destructive method for the estimation of biomass requires allometric equations of forest tree parameters such as tree Diameter at Breast Height (DBH), crown projected area (CPA), and height (Chave et al., 2014; (Kenzo et al., 2009). Studies have used remotely sensed data for the retrieval of forest parameters and subsequently mapping of biomass (Tsui, Coops, Wulder, Marshall, & Mccardle, 2012; Zarco-Tejada, Diaz-Varela, Angileri, & Loudjani, 2014).

Many studies have used radar technology for the estimation of tree parameters and biomass (Carreiras, Melo, & Vasconcelos, 2013; Morel et al., 2011; Suzuki, Kim, & Ishii, 2013). RADAR is an active remote sensing technique that uses radio waves to determine the range of objects. Despite its potential, radar technology is expensive and not readily available. Moreover, studies have found its sensitivity to biomass saturation levels (Rodríguez-Veiga, Wheeler, Louis, Tansey, & Balzter, 2017). Also, radar system characteristics, topography, and characteristics of the material being imaged influences the intensity return back to the sensor. These limitations affect its ability to provide information on the object being studied.

Terrestrial Laser Scanner TLS is also an active sensor that works by sending and receiving emitted laser pulses from the target. Occlusion effect has been emphasised as one of the limitations of the TLS in a heterogeneous forest stand (Moskal & Zheng, 2011). Also, plot-based scans, portability issues and laborious of the TLS system has also been recognised (Gatziolis, Lienard, Vogs, & Strigul, 2015). The reasons aformentioned, limit the use of TLS for accurate retrieval of forest parameters.

A lot of research has also been conducted using high resolution multispectral bands satellite imagery such as IKONOS, World-view and Quick bird (Kim, Im, Do, Kim, & Joo, 2016; Mbaabu, Hussin, Weir, & Gilani, 2014). Multispectral images have the major shortcoming of cloud cover obscuring the observations of the land surface (Rodríguez-Veiga et al., 2017). Most importantly, these images do not provide information on the vertical structure of forests (García, et al., 2010).

Light Detection and Ranging (LiDAR) is an active sensor that provides 3-dimensional models used to derive forest tree height (Hunter, Keller, Victoria, & Morton, 2013; Næsset & Økland, 2002; Nie, Wang, Zeng, Xi, & Li, 2017; van Leeuwen & Nieuwenhuis, 2010). However, LiDAR is an expensive technology.

The Unmanned Aerial Vehicle (UAV), is an inexpensive and portable platform. It enables to capture imagery of high spatial and temporal resolutions, hence allows the identification of small objects in details. The images are free of occlusions, clouds, and fewer shadows that surpasses the limitations of other satellite borne data (Tomaštík, Mokroš, Saloš, Chudỳ, & Tunák, 2017). In actuality, it is a cost-effective technology that provides a new dimension in aerial photography, ecosystem mapping and monitoring.

Structure From Motion (SFM), defines the method of generating three-dimensional structure from two-dimensional images. This is achieved by stereo vision; whereby images are captured from different position with a percentage of overlap. Afterwards, depth information is calculated by parallax (positional difference between images taken from different position) (Lim, Ye Seul La, Phu Hien Park, Jong Soo Lee & Pyeon, Mu Wook Kim, 2015). Therefore, applying the Structure from motion photogrammetric technique on images captured by UAV, reconstruction of the imagery can be used to generate point cloud data that is comparable to ALS derived point cloud (Puliti, Olerka, Gobakken, & Næsset, 2015; Tomaštík et al., 2017; Wallace, Lucieer, Malenovsk, Turner, & Petr, 2016). Research has shown the use of imagery taken by UAV to generate 3-D point cloud through photogrammetric image matching and processing (Harvey, Rowland, & Luketina, 2016; Lisein, Pierrot-Deseilligny, Bonnet, & Lejeune, 2013). From the photogrammetric processing, ortho-mosaic images, Digital Terrain (DTM) and Digital Surface Model (DSM) are obtained (Bendig et al., 2015; Zarco-Tejada et al., 2014). The DSM is subtracted from the DTM to derive the Canopy Height Model (CHM) for the extraction of tree height.

1.2. Unmanned Aerial Vehicle

UAV is an acronym for Unmanned Aerial Vehicle (UAV), also known as Unmanned Aerial Systems (UAS), drone or Remotely Piloted Aircraft (RPA). In the past, UAV was originally developed for military applications, and since the 1950's, UAV has been used for aerial surveillance (Tang & Shao, 2015). Recently, the use of UAVs for civil applications has gained tremendous recognition (Shahbazi, Théau, & Ménard, 2017).

According to Anderson & Gaston, (2013), UAV is generally categorised into two types; fixed wing platforms and rotor based copter systems. These systems differ in terms of their flying altitude, size, and range of data coverage. These distinctive characteristics often define the applications that can be supported by each class of the UAV category.

The fixed wing platforms can travel at a faster speed and cover a large area. On the other hand, the rotor based systems fly at slower speed, cover a smaller area and are also smaller in sizes as compared to the fixed wing systems.

1.3. Airborne Laser Scanner

LiDAR sensor operates in the near infrared and blue region of the electromagnetic spectrum. It possesses three technologies that enable it operations; Laser ranging for accurate distance measurement; Differential Global Positioning System (DGPS) for satellite positioning and Inertial Measurement Unit (IMU) to record orientation. Airborne LiDAR operating principle is shown in Figure 1.

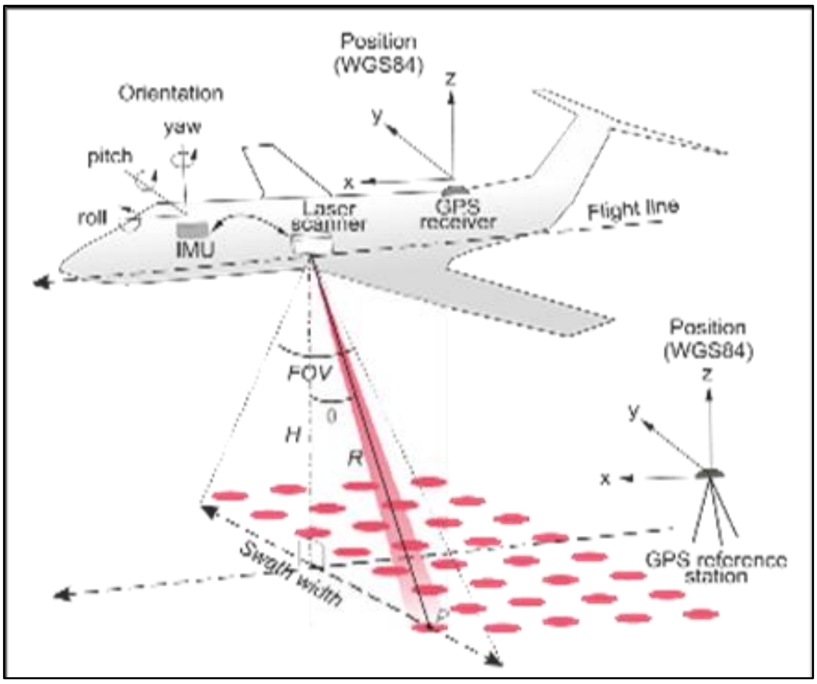

Figure 1: Airborne Lidar operational system
Source: (Gallay, 2013)

Lidar systems capture information about their target by ranging followed by accurate measurement of the time between the emission of the laser pulse from the sensor to the target and the received reflections from the target back to the sensor. Based on this, LiDAR provides elevation data points also referred to as 3-dimensional point cloud data.

The use of LiDAR technique for forest inventory purposes began in the 1980s. Nevertheless, LiDAR remote sensing had already been used for the creation of Digital Elevation Models (DEMs) and the retrieval of atmospheric particle concentrations (Ritchie, 1996). In the forestry domain, LiDAR data is used to derive information on forest tree height. (Hunter, Keller, Victoria, & Morton, 2013; Næsset & Økland, 2002).

1.4. Overview of previous related research

Tree height is the vertical distance between the base to the highest point of the tip. Forest tree height can be obtained from the surface differentiation of the DSM and DTM (Figure 2). The DTM and DSM are input for the creation of a forest Canopy Height Model. The retrieval of tree height using remote sensing techniques is dependent on the accuracy of the modelled terrain.

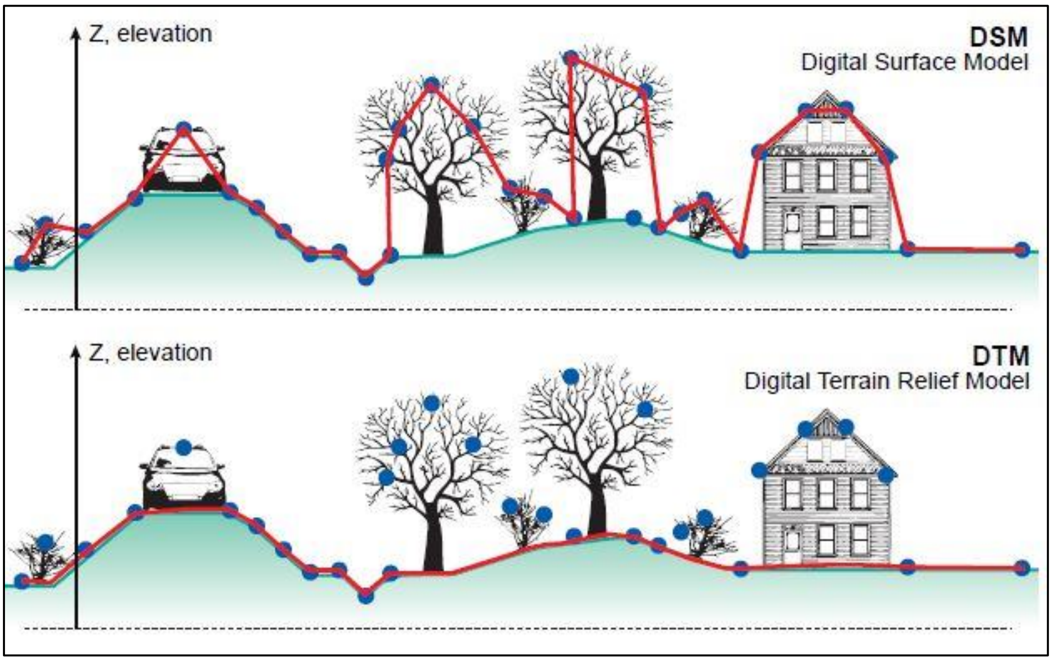

Figure 2: Illustration of DSM and DTM

http://www.charim.net/sites/default/files/handbook/datamanagement/3/3.2/DSMDTM_1.JPG

Assessment of this 3D model has been done conducted by research. Andersen et al., (2003), modelled tree height by comparing DTM sourced from Airborne LiDAR, Interferometric Synthetic Aperture Radar (InSAR) and aerial photos oriented within an analytical stereo plotter. Validation of the 3D models was done by elevation data collected at regular intervals within the study area. The results of the study proved that DTM produced from LiDAR is more accurate, while InSAR and aerial photos underestimated tree height. Reuben, (2017), estimated forest tree height by comparing the accuracy of ALS and UAV derived DTM to the reference elevation points collected using a Differential Global Positioning System (DGPS). The accuracy of the LiDAR sourced DTM was 1.25m while UAV obtained DTM had an accuracy of 3.84m. In the same view, Okojie, (2017), retrieved tree height by comparing the DTM derived from airborne LiDAR and UAV data in a temperate forest. Also, the accuracy of the 3D models was done using elevation points collected using a DGPS. The image matching UAV derived terrain model had an error of 0.53m, while LiDAR DTM had an error of 2.45m. Additionally, Gbenga Ajayi, Anthony Salubi, Fredrick Angbas, & Godfrey Odigure, (2017) appraised the vertical and horizontal error in a DTM utilising stereo images captured using UAV in an urban environment. The horizontal and vertical accuracies were 0.0467m and 0.1151m respectively when compared to elevation data acquired using Hi-target DGPS.

The crown projection area (Figure 3) of a tree is the area of the vertical projection of the outermost perimeter of the crown on the horizontal plane (Gschwantner et al., 2009).

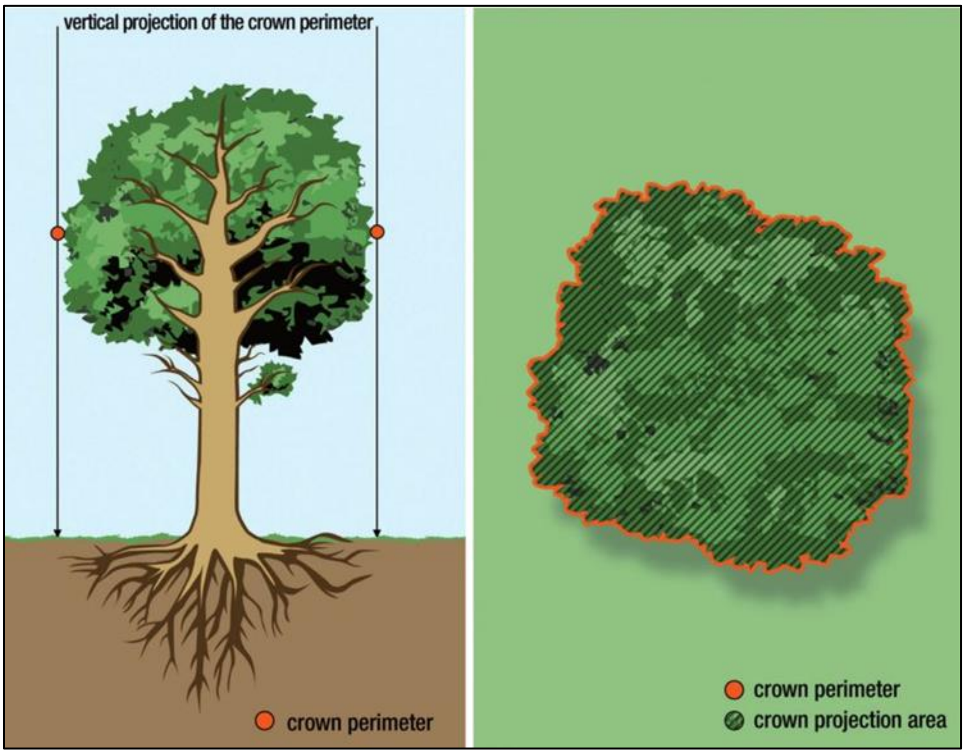

Figure 3: Crown projection area

Research has been done to establish the relationship between the tree CPA and Diameter at Breast Height (DBH). Baral, (2011), used Object Based Image Analysis (OBIA) to delineate tree crowns on Geo-Eye and Worldview-2 data to obtain CPA in the subtropical rainforest in Chitwan, Nepal. Modelling of the relationship between the CPA and DBH found a nonlinear relationship existing between the variables.

Also, Karna et al., (2015), extracted CPA from Worldview-2 optical data to model the relationship between DBH. Their study found a linear relationship existing between CPA and DBH of tree species.

1.5. Problem statement

The use of cost-effective approaches for estimation of forest biomass is the requirement for an effectual Monitoring, Reporting and Verification (MRV) within the REDD+ programme (Gizachew & Duguma, 2016). Forest biomass estimation using remote sensing method employs tree biophysical parameters such as Diameter at Breast Height (DBH), tree height and crown projected area (CPA).

Tree height is one of the essential forest parameters used in the allometric modelling of biomass (Andersen, Reutebuch, & Mcgaughey, 2006). The addition of this variable significantly improves the accuracy of biomass estimation, compared to the sole use of DBH (Hunter et al., 2013).

Tree height can be measured in the field based on visual interpretation. However, this method is often biased because of difficulty in visibility caused by intermingling tree crowns (Chave, 2005; Khatry Chhetri & Fowler, 1996). Therefore high uncertainties arise in field based measurement of tree height (Calders et al., 2015; Molto, Rossi, & Blanc, 2013). Hence, remote sensing techniques became an alternative, effortless method to derive forest tree height (Edson & Wing, 2011; Tao et al., 2014). The use of this method is dependent on the accuracy of the modelled tree height (Reutebuch, et al., 2003). Ensuring accuracy is paramount because errors in the modelled tree height can influence the biomass values.

However, many of the research has been done in temperature region and open forests. The accuracy of modelling tree height comparing LiDAR and UAV derived data is not well established in the tropical rainforest. There is need to investigate the performance of these datasets in a tropical rainforest with complex and dense canopy density. In this regards, an investigation on the performance of this two technology for the estimation of forest canopy height needs to be assessed.

Another forest parameter of interest is the tree Diameter at Breast Height. Although this parameter cannot be extracted using remote sensing methods, it found to be correlated with the crown projection area (CPA) (Shimano, 1997). The crown projection area can be retrieved from the delineation of tree crowns on an orthophoto through the implementation of image segmentation. The orthophoto obtained from photogrammetry processing of UAV acquired images can be employed to extract this parameter. The use of the orthophoto is required because of it high spatial resolution and to overcome the cloud contamination which is characteristic of optical images in the tropical climate (Tomaštík, et al., 2017).

1.6. Research objectives

1.6.1. General objective

The overall aim of this study is to assess the performance of UAV derived data to extract forest parameters and estimation of aboveground biomass in Berkelah Tropical Rainforest, Malaysia.

1.6.2. Specific objectives

The specific objectives are divided into three sub-groups.

- Canopy Height Modelling.
  1. To assess the accuracy of DTM from airborne LiDAR and UAV sourced stand-alone datasets as compared to GNSS points.
  2. To compare the tree height estimated from the Canopy Height Models generated from airborne LiDAR and UAV datasets.
- Modelling the relationship between crown projection area and Diameter at Breast Height
  1. To model the relationship between crown projection area and field measured Diameter at Breast Height (DBH).
- Allometric modelling of the forest aboveground biomass.
  1. To estimate aboveground forest biomass of forest trees from field measured and predicted Diameter at Breast Height in combination with the most accurate tree height within the study area.

1.7. Research questions

- Canopy Height Modelling
  1. What is the segmentation accuracy of tree crown delineated from the orthophoto?

ii. What is the accuracy of the DTM from airborne LiDAR and UAV sourced stand-alone datasets as compared to the GNSS points?

iii. What is the difference in the tree height estimated from the Canopy Height Models generated from airborne LiDAR and UAV datasets?

- Modelling the relationship between crown projection area and Diameter at Breast Height
  i. What is the relationship between crown projection area and field measured Diameter at Breast Height?
- Allometric modelling of forest aboveground biomass.
  i. What is the difference in the aboveground forest biomass estimated from field measured and predicted Diameter at Breast Height in combination with tree height within the study area?

1.8. Research hypothesis

- Canopy Height Modelling
  i. H_o: DTM generated from UAV stand-alone dataset possess a higher RMSE than DTM generated from airborne LiDAR dataset.
  Ha: DTM generated from UAV stand-alone dataset possess a higher RMSE than DTM generated from airborne LiDAR dataset.
  ii. H_o: There is no significant difference in tree height modelled using Canopy Height Models generated from airborne LiDAR and UAV stand-alone datasets.
  H_a: There is a significant difference in tree height modelled using Canopy Height Models generated from airborne LiDAR and UAV stand-alone datasets
- Modelling the relationship between crown projection area and Diameter at Breast Height
  i. H_o: There is no significant relationship between crown projection area and field measured Diameter at Breast Height.
  Ha: There is a significant relationship between crown projection area and field measured Diameter at Breast Height.
- Allometric modelling of forest aboveground biomass
  i. H_o: There is no significant difference between aboveground biomass estimated from field measured and predicted Diameter at Breast Height in combination with the tree height within the study area.
  Ha: There is a significant difference between aboveground biomass estimated from field measured and predicted Diameter at Breast Height in combination with tree height within the study area.

2. DESCRIPTION OF STUDY AREA AND DATA USED

2.1. Geographical location

This study was carried out in the Berkelah Tropical Rainforest Reserve, located in Maran District, in the state of Pahang, Peninsular Malaysia (Figure 4). It lies between latitude 2°35' and 3°60'N and longitude 100°45' and 102°00'E (Rajpar & Zakaria, 2014).

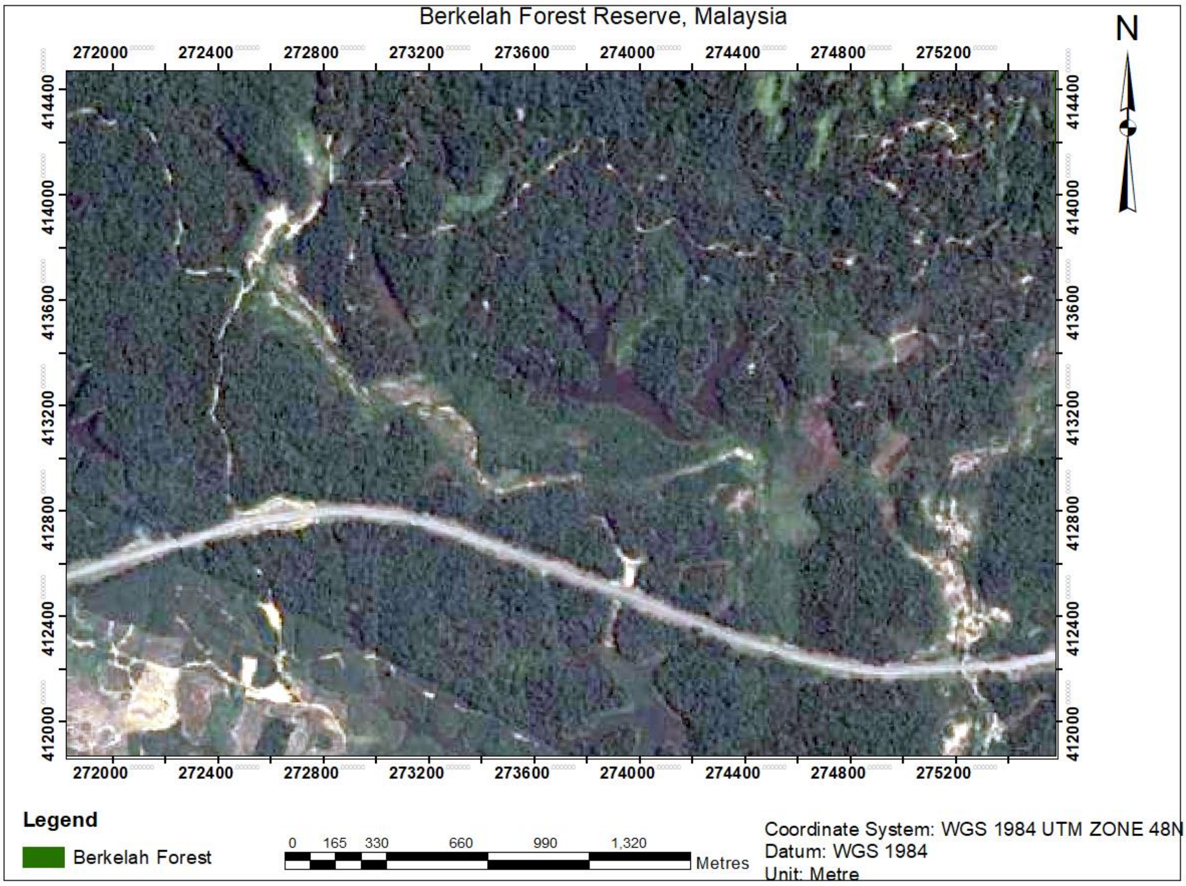

Figure 4: Image of study area

2.1.1. Climate

The climate is classified as tropical. On the average, the annual temperature is 26.7 °C, with minimum and maximum temperature of 25.6°C and 42.2°C respectively. The average precipitation is 2866mm annually.

2.1.2 Vegetation

The vegetation in the Berkelah Forest Reserve is characterized as Hill Dipterocarp Lowland Tropical Rainforest, comprised of different aged post-harvest trees. Abundant tree species are present within the forest, with the dominant species belonging to the family Dipterocarpaceae (Bing, Rajpar, & Zakaria, 2013).

2.2. Materials

2.2.1. Field equipment

Different field instruments were used to measure forest tree parameters during the fieldwork. Table 1 shows the enumerated field instruments and the use

Table 1: List of field instrument and uses

Instrument	Use
iPAQ	Navigation and recording coordinates of trees
Measuring tape	Outlining of plots
Diameter tape	Measurement of tree DBH
Spherical densitometer	Measurement of canopy density
Field data sheets	Recording of field data
First aid kit	For emergency treatment

2.2.2. Processing software

Different software were used for the execution of thesis work. The processing software and their use are listed in Table 2 below.

Table 2: List of software and their use

Software	Use
ArcGIS 10.5.1	Data processing and visualisation
Pix4D	Photogrammetry processing
eCognition	Tree crown delineation
LaStools	ALS data processing
MS Office 2016 (Excel)	Statistical analysis
R Studio	Statistical analysis
MS Office 2016 (Word)	Reports and thesis writing
Mendeley Desktop	Citation and references

2.3. Data

2.3.1. Biometric data

Forest tree parameters were the biometric data used for this study. The data were collected during field work using the instruments listed in Table 1.

2.3.2. UAV derived data

The stereo images were acquired using Phantom 4 DJI UAV. The acquired stereo images were used to generate photogrammetric products namely; DTM, DSM and ortho-mosaic. The images were obtained on the 29th, 30th of September and 10th of October 2017.

2.3.3. Airborne laser scanner data

The Airborne LiDAR data used was provided by the MARA University of Technology (UiTM), Selangor, Malaysia. It was acquired on the 14th November, 2014 by the Airborne Research and Survey Facility Airborne Research and Survey Facility's (ARSF) work of the Natural Environment Research Council (NERC) Gloucester, UK. The data was recorded in discrete return LiDAR systems and supplied as ASCII and LAS 1.2 point cloud format, with an average point density of 5point per m^2. The point cloud data contains X Y Z coordinates, intensity, classification, return number, number of returns for given pulse and scan angle rank. The data was captured in 22 subsets (flight lines), however, due to data quality, only 20 flight lines were processed and used for further analyses.

3. METHODOLOGY

3.1. Research methods

The research method in this study is comprised of five parts;

1. The first part was biometric data acquisition and processing; which involved field observation and tree parameters collection using field instruments listed in Table I of the previous chapter. After completion of the field work, the biometric data was analyses.
2. The second part was the stereo imagery acquisition; The UAV platform was used to acquire the stereo images. The images were processed using Pix4D to derive the DSM, DTM and orthophotos
3. The third part was the Object Based Image analysis; The orthophoto was delineated using eCognition software to derive tree crown projection area (CPA). The CPA was used to model relationship between field measured DBH.
4. The fourth part was DTM generation and accuracy assessment; The DTM created from the UAV and LiDAR data were evaluated in relation to the GNSS points.
5. The fifth stage was the generation and estimation of tree height and comparison; Tree height was extracted from the CHM of UAV and LiDAR and comparison between the height variables was done. Finally, aboveground biomass was estimated and compared between field DBH and predicted DBH in combination with the retrieved forest tree height. The workflow is summarised in the flowchart shown in Figure 5.

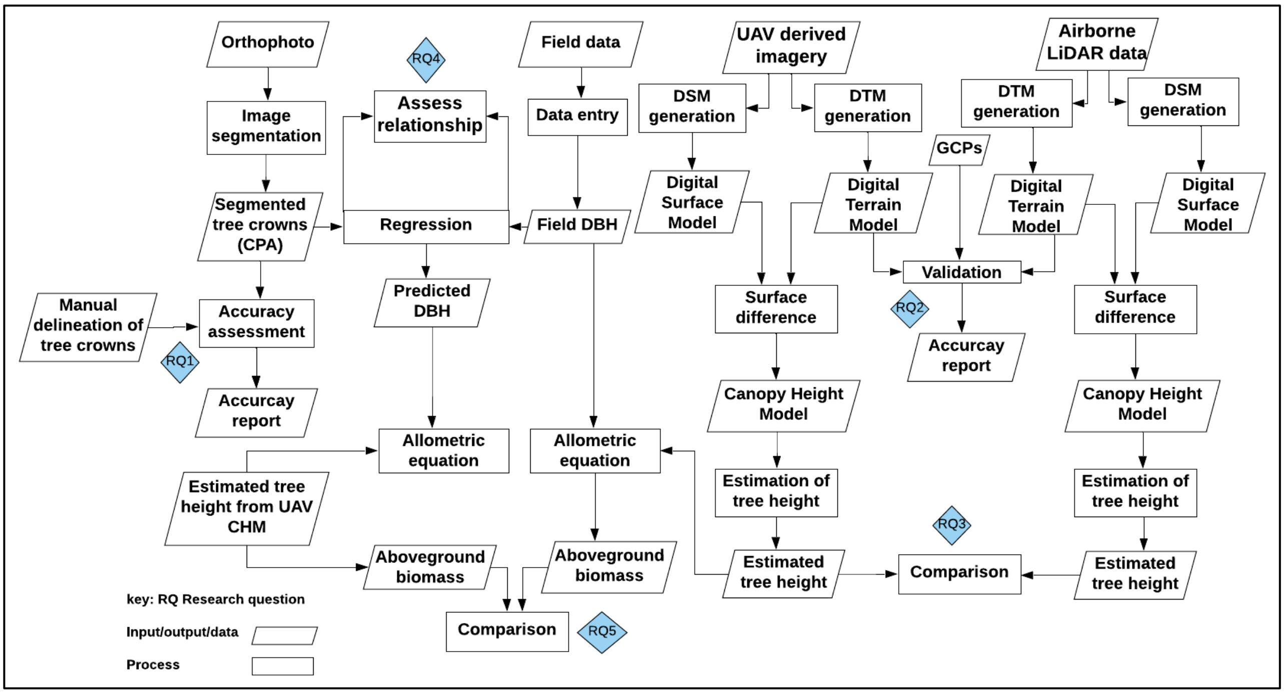

Figure 5: Flowchart of the methodology

The research methodology is summarised in the flowchart shown in Figure 5 below.

The study was conducted in three study sites or blocks within the Berkelah forest. The same process was applied for the data processing and data analyses of all sites. Hence the flowchart above summarises the methodological steps for the three study sites.

3.2. Biometric data

Tree biophysical parameters were the biometric data employed during the course of this study. The field data and method of collection are discussed in the following subsections.

3.2.1. Sampling design

Purposive sampling design was used for data collection in the field. This sampling design was used due to accessibility of the forest. Purposive sampling is a non-probability sampling method based on the judgement of the researcher. Also, the sampling design was used to by taking into consideration the areas flown by the UAV during data acquisition of the stereo images. The flight areas were selected based on the availability of open spaces for placing ground control points and to incorporate the different variations in forest structure present in the study location. Hence, the plots were selected to include the areas covered by the UAV flight. Each plots were sampled with a distance of over 50 metres apart. Figure 6 shows the study area map with sample plots and three study sites (area covered by the UAV) within the forest.

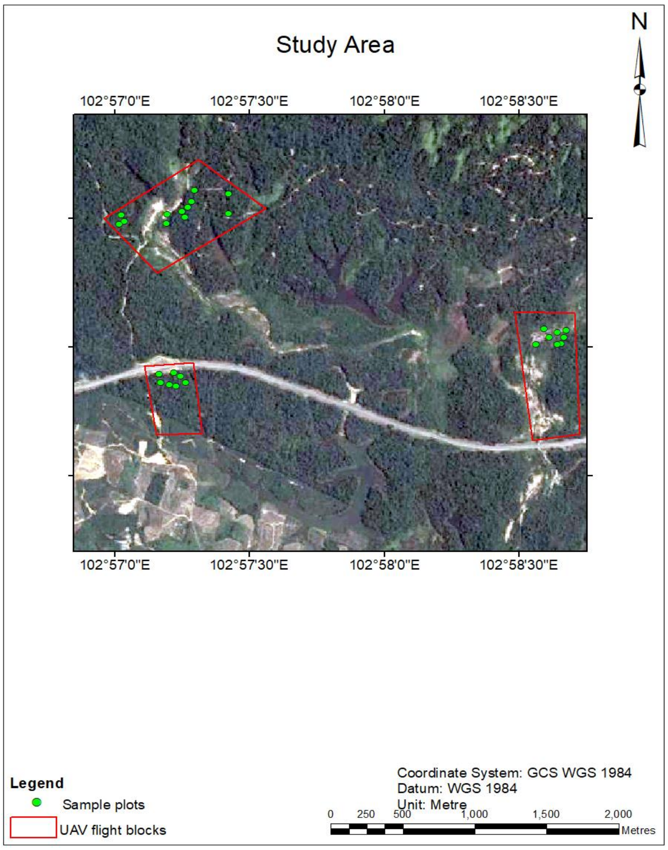

Figure 6: Study area map showing UAV flight blocks and sample plots

3.2.2. Plot size

Mauya et al., (2015), emphasized the advantages of circular plots over other plot types, because of the ease of outlining and less prone to errors in the plot area as compared to rectangular and square plots. For these reasons, the circular plot was used for in this study. The plot size of 500m² which is equivalent to radius of 12.62metres was used for forest inventory parameters acquisition. In a study done by Ruiz, et al., (2014), revealed that increasing plot size beyond 500m² does not significantly improve the result of AGB estimation. Instead, it would require more trees to be sampled at each plot thereby increasing cost and time.

3.2.3. Biometric data collection

Field data was collected between September and October, 2017. Fieldwork was conducted to acquire forest biophysical parameters. After delineation of plot size and an indication of tree numbers with tags, Diameter at Breast Height was measured using diameter tape. According to Brown, (2002), trees with Diameter at Breast Height less than 10cm contribute less to the total biomass and carbon of a forest. Live trees (living trees) with DBH of above 10cm measured at 1.30cm above the ground were only measured. For consistency, a DBH stick was used to measure the DBH at 1.30m. In addition, the coordinate of trees and the centre of the plots of all sample plots were recorded in the iPAQ. Figure 7 shows data collection in the field. All the measured tree parameters were recorded on the data collection sheets and transferred to Microsoft Excel for further analyses. The datasheet is shown in Appendix 1.

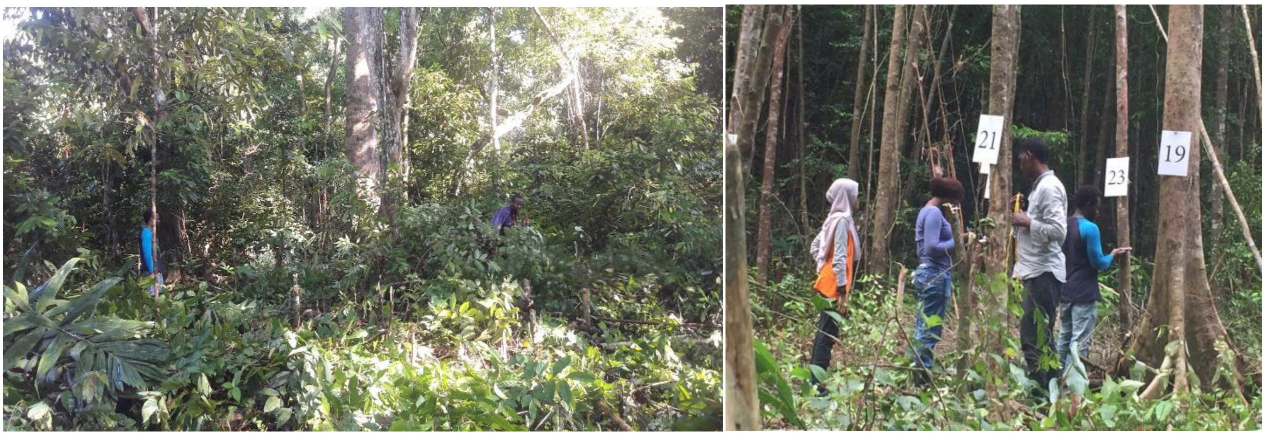

Figure 7: Sample plot before and after clearing the undergrowth and placing tree tags for biometric data collection

3.3. Data acquisition using UAV

3.3.1. Mission planning

The PiX4D capture software was used to define the parameter for the flight. The spatial quality of the ortho-mosaicked images depends on flight height and percentage of overlap. Dandois, Olano, & Ellis, (2015), assessed the relationship between optimal flight altitude, overlap, weather conditions for UAV data acquisition and quality of the point cloud in a forest ecosystem. The study clinched that higher point density, proper alignment and image matching in the photogrammetry processing is highly correlated with an increase in forward and side overlap and flight height. To ensure high quality of the photogrammetry outputs, an overlap of 90m, and height of 110m above the ground were used for image acquisition. The speed of the UAV also has an effect on the images, to avoid blurred images moderate speed was adopted. Image acquisition parameters of the data are shown in Table 3.

Table 3: UAV data acquisition parameters

Parameter	Value
Altitude	110m
Angle	Nadir (90)
Front overlap	90%
Side overlap	70%
Speed	Moderate

3.3.2. Allocation of Ground Control Points

Ground control points were allocated to aid spatial georeferencing of the photogrammetry outputs. The GCPs were well distributed at the edges of the flight areas using a black and white spray paint, this was done to ensure visibility for the UAV during data capturing and to be discernible on the images during georeferencing. The distribution of the GCPs at the edges of the flight area helps to avoid distorted images during photogrammetric processing. The minimum number of ground control points for georeferencing an image is three. Francisco Agüera-Vega, Fernando Carvajal-Ramírez, & Patricio Martínez-Carricondo (2017), analysed the influence of varying the number of GCPs for georeferencing on the accuracy of the Digital Surface Models, Digital Terrain Models, and ortho-mosaic. Their study revealed that increasing the number of GCPs increases the accuracy of the DSMs, DTMs and ortho-mosaic. In light of the above, minimum of 6 GCPs were used for placing ground control points. Afterwards, the control points obtained in X, Y and Z, were recorded with a Differential Global Positioning System.

3.3.3. Image acquisition

After the placement of GCP's, the images were captured based on the defined parameters (overlap, height, speed). The resultant images were stored in a memory card.

3.3.4. Photogrammetry processing

The acquired images were processed using PiX4D software to derive DSM, DTM and rthophotos. The photogrammetric workflow in PiX4D are divided into three stages:

- Initial processing

This stage involves the computation of key points, image matching and camera calibration (Pix4D, 2017). It commences with the creation of a new project and loading the images into the software. The UAV collects collect hundreds of images of the area and to create one scene, the software first compute the keypoints. The keypoints in adjacent images based on same location are used to match the images together. Then, the camera calibration and generation of sparse point were done. Afterwards, the GCPs were loaded into the software, and control points were marked on the images and the process of re-optimization of the images was carried out by the software.

- Point cloud densification

This stage increases the density of the 3D points computed from the former stage. Densification of the sparse point cloud increases the accuracy of the Digital Surface Model and orthophotos that will be generated subsequently. The point cloud classification option was chosen, which according to (Pix4D, 2017), it improves the accuracy of DTM.

- DSM and orthomosaic generation

This stage computes the generation of the DSM and orthomosaic from the densified point cloud done at the second stage. The computation of the point cloud can result in noise and erroneous points. To correct for this, the noise filtering option was chosen. Also, the generation of the DSM is dependent on the point cloud, this surface can contain areas with inaccurate small bumps. The surface smoothing utilising the sharp option was chosen to smoothens the resultant DSM. After that, the DSM was generated by interpolation using a Delaunay triangulation method. The triangulation algorithm was chosen as recommended by (Pix4D, 2017), because of its suitability for forest ecosystems. Finally, the orthomosaic was generated from the mosaicking of the geometrically corrected images. The merge tiles option was checked to create a continuous and complete scene of the DSM and Orthomosaic. The photogrammetry outputs are shown in Table 4.

Table 4: Photogrammetry processing outputs

Processing outputs	**Site 1**	**Site 3**	**Site 3**
Area	72.1ha	46.69 ha	74.64 ha
Georeferencing (RMSE)	0.27m	0.30m	0.04m
Ground sampling distance	4.85 cm	5.16 cm	4.86 cm
Number of 3D Densified Points	70081738	33708414	71368890
Average point cloud/m3	27.39	13.83	26.3
Mean reprojection error	0.183	0.208	0.164

The reprojection error measures the geometric error of the distance between a projected point (3D point) computed from the photogrammetry and the measured 3D point.

3.4. Object Based Image analysis

Image segmentation is one of the processes in the object based image analysis (OBIA). It is the process of partitioning an image into a number of homogeneous segments or units based on a given criteria (Fan, Zeng, Body, & Hacid, 2005). Image segmentation was done to delineate the orthophotos to obtain objects of interest; crown projection area using multiresolution algorithm. Multiresolution is a bottom up region based segmentation process, that is starting with one pixel object, and iteratively, smaller objects were merged into larger ones (Drăguţ, Tiede, & Levick, 2010). Scale, shape and compactness are criteria used to segment objects into homogenous units within the multiresolution algorithm. This algorithm was used to because it has been proven to delineate homogeneous objects at different resolutions.

- The scale parameter determines the size of objects that are segmented in the multiresolution algorithm. It also determines the maximum allowable heterogeneity in the segmented objects. Higher scale parameter leads to larger and less homogeneous objects by increasing the threshold of heterogeneity per object (Drăguţ et al., 2010).
- The shape criterion determines the influence of spectral value on the heterogeneity of the segmented objects. It is characterised by two parameters: smoothness and compactness. The smoothness enhances the smoothness of the borders of the image objects, and the compactness determines the compactness of the segmented objects.

The orthophotos were captured in the RGB band of the electromagnetic spectrum. Therefore all image layers had the same influence in the segmentation process. Selection of optimum criteria (scale, shape and compactness) for segmentation is dependent on trial and error approach. Therefore the scale, shape and compactness values were adjusted iteratively until image objects of interest was achieved.

3.4.1. Removal of shadows and non-vegetated areas

The next step was to distinguish between vegetated and non-vegetated objects. Classification and removal of unwanted objects are possible using the image object information such as (brightness, standard deviation, maximum difference and mean etc.) within the eCognition software. These image object information are dependent on threshold values. The first step was to remove shadows, utilizing the brightness image object information. The maximum difference was used to classify road features, while standard deviation was used to classify the waterbody present within the objects of interest; tree crowns. After successful classification of unwanted features, the merge region algorithm was used to merge all unwanted(non-vegetated) objects to create a large continuous objects.

3.4.2. Watershed transformation

Watershed transformation is an algorithm to separate clusters of tree into individual trees. The algorithm considers the image as a topographic surface and uses the local minima, catchment basins and watershed lines (dams) to operate. To implement the process, the image which is considered as a topographic within this algorithm, gets flooded from it minima, and dams are built to prevent water coming from two different

catchments basins to merge into one catchment basin. (Drăguţ et al., 2010). The watershed mechanism is illustrated in Figure 8. Using this algorithm, clusters of tree were separated into individual trees.
The algorithm is dependent on threshold value (length factor). The size of the largest tree crown observed during fieldwork was 10m. Therefore, 33 pixels were used as the length factor (threshold value) were I pixel of image resolution is 0.3m. Based on the given threshold, cluster of trees were separated to form one new segment, at iterations.

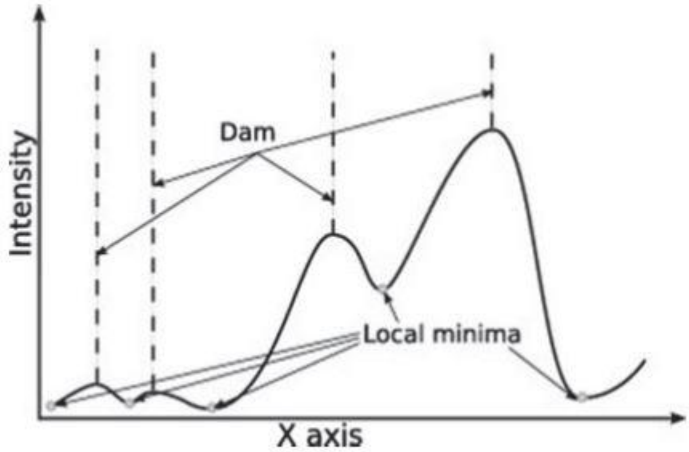

Figure 8: Illustration of watershed transformation algorithm
Source: (Derivaux et al., 2010)

3.4.3. Morphology

Morphology reshapes and polishes the resultants tree segments, and make the crowns to be round as trees would appear in real life. To achieve this, a circular mask width of 10 was used. The value 10 is dependent on the largest tree crown observed in the field. Within the morphology interphase, the close image objects option was chosen, the close image objects adds pixels from outside the segment based on the threshold of the circular mask width.

3.4.4. Removal of undesired objects

This was done in two steps. The first was done to remove asymmetrical and elongated shaped objects using the image object information of geometry (roundness). Subsequently, all trees with pixels ≤ 22 was used to remove tree crowns less than 2m². The remaining segments were exported as .shp format to ArcMap for validation of segmentation.

3.4.5. Accuracy assessment of segmentation

The validation of image segmentation was done by comparison of polygons obtained from the OBIA and manually segmented polygons. Different approaches for the validation of image segmentation, have been used by researchers. Möller et al., (2009), used the relative area of intersection between segmented objects and reference objects. Gougeon, (1995), used 1:1 spatial correspondence between segmented objects and reference objects to mention but a few. However, Clinton, et al., (2010), assessed different approaches employed by researcher for the accuracy of segmentation. The study modified the method introduced by (Möller et al., 2009) that uses used the relative area of intersection between segmented objects and reference objects. The validation of segmentation was done using an area based measure adopted after (Clinton et al., 2010).

To achieve this, the reference objects were manually delineated on the orthophoto based on visual image interpretation. To ensure consistency in the manual digitization of tree crowns, the digitization was done at a scale of 1: 250. Afterwards, spatial join of the reference and automatic segmentation was done in ArcGIS. The validity of the segmentation was calculated by oversegmentation, under segmentation and D value.

- Oversegmentation model is described in equation 1.

Equation 1: Oversegmentation equation

$$Over\ segmentation_{ij} = 1 - \frac{area\ (Xi \cap Yj)}{area\ (Xi)} \ \ldots\ldots\ldots\ldots\ldots\ldots 1$$

Source: (Clinton et al., 2010)

- Undersegmentation model is described in equation 2

Equation 2: Undersegmentation equation

$$Under\ segmentation_{ij} = 1 - \frac{area\ (Xi \cap Yj)}{area\ (Yj)} \ \ldots\ldots\ldots\ldots\ldots\ldots 2$$

Source: (Clinton et al., 2010)

Where;

xi Reference object manually segment tree crown (On screen digitized objects)

yj Corresponding segmented object by eCognition

Oversegmentation and undersegmentation values ranges between 0 and 1.

- The total error detected in the segmentation shown in equation 3.

Equation 3: Measure of goodness

$$D = \sqrt{\frac{over\ segmenation^2 + under\ segmenation^2}{2}} \ \ldots\ldots\ldots\ldots 3$$

Source: (Clinton et al., 2010)

From the total error detected in the segmented, we inferred the accuracy of the tree crown segmented

3.5. Airborne LiDAR Processing

The LiDAR data was processed to generate the DSM and DSM. The DTM is a 3-dimensional representation of the bare earth surface, while the DSM is a 3-dimensional representation of the objects on the earth surface including the bare earth. The point cloud was classified into four returns, where the last return represents the DTM and first return represents the DSM. DTM was produced from the interpolations of the last return using a cell size of 1m. Also, the DSM was generated through interpolation of the first return of the point data using a cell size of 1m.

3.6. Digital Terrain Model accuracy and comparison to the GNSS points

The Pix4D enables the generation of a DTM from the photogrammetry output. So the UAV derived DTM and the ALS derived DTM were assessed for their accuracies. To evaluate their accuracies, the GCPs were overlaid on the DTM, and the extract raster to point feature in ArcGIS was used to retrieve the elevation of the DTM and this was compared to the height values measured with DGPS in the field. The root mean square error (RMSE) was used to compute the deviation of the dependent variable (DTM) along the line of fit (GNSS Z-values). The equation of the RMSE is shown in equation 4 below.

Equation 4:RMSE formula

$$\text{RMSE} = \sqrt{\sum_{i=1}^{n} \frac{(Y_i - Y'_i)^2}{n}}$$

Source: Chai & Draxler, (2014)

Where;

RMSE; Root Mean Square Error

yi; Measured variable of the dependent variable; elevation (z) values measured in the field

Ŷi; Predicted variable of independent variable; elevation (z) values retrieved from DTM

n; Number of observations counted/number of points

3.7. Generation of Canopy Height Models

The extraction of tree height requires the Canopy Height Model. The CHM represents the tree height values as a continuous surface and the DTM and DSM serve as the input data. The CHM was created in ArcGIS software. For ease of comparison of the height variables, the DTM and DSM from both data were generated using a grid size of 1m, so the resultant CHM also have same resolution. Surface differentiation of DTM and DSM using raster calculator in ArcGIS was used to obtain the CHMs from the UAV sourced and ALS data. Afterwards, tree height were extracted from each CHM.

3.8. Estimation of tree height from the Canopy Height Models

One of the ways to retrieve tree height from the CHM is image segmentation (Barnes et al., 2017). Estimation of the tree height from the CHMs. To accomplish this, the shapefiles of the segmented tree, the coordinate of trees recorded in the field, the centroid of the plot and circular plot were overlaid on each of the CHMs, and the highest pixel value of the CHM within the segmented individual tree crown was retrieved as tree height. This was done on a plot basis starting first with one study site, and then the same process was applied to the other study sites.

3.9. Statistical and data analyses

The histogram was used to graphically determine the distribution of the field measured DBH.Correlation was used to quantify the strength of relationship between the CPA and DBH.

Regression is used to model the relationship between dependent and independent variable. The changes in independent variable results in change of the dependent variable, hence there is a cause and effect relationship. Regression analyses was established between CPA and DBH, using CPA as the predictor and field DBH as the response variable. The relationship between the variables were analysed using simple and nonlinear regressions. Also regression was used to ascertain the relationship between estimated tree height from the LiDAR and UAV CHMs. The estimated tree height from the UAV CHM was taken to be the independent variable because it was found to have least errors in the DTM.

Finally, t-test was used to compare the modelled tree height from CHMs of LiDAR and UAV. T-test was also used to compare the aboveground biomass modelled using predicted and observed DBH with the retrieved tree height from UAV CHM.

3.10. Estimation of Above Ground Biomass

Allometric equations are used to describe the relationships between one or more parts of a tree to another. The above ground biomass was calculated using allometric equation. There exist many allometric equations in published literature. However, this study used the equation proposed by (Chave et. al., 2014), which is applicable in tropical rainforest. The formula is shown in equation 5 below.

Equation 5: Allometric equation for estimating aboveground biomass

AGB = 0.0673 * (ρ D2 H)0.976

Where:

AGB is aboveground biomass estimated in Kilogram

D is diameter at breast height in centimetre

P is wood density in grams per cubic meter (gcm3)

H is tree height in metre

0.0673 and 0.976 are constants

3.11. Estimation of carbon stock

The carbon stock of each tree was calculated from the AGB value. A conversion factor of 0.47 was applied to estimate carbon stock from the AGB values using equation 6. This is based on the idea that biomass contains 50% of carbon.

Equation 6: Carbon equation

$$C = B * CF$$

Where: C is the carbon stock in tons

B is the dry biomass

CF is the carbon fraction (0.47)

4. RESULTS

4.1. Biometric data

Tree Diameter at Breast Height (DBH) was recorded for 769 trees collected from 32 plots in the study area. The results of the descriptive statistics analysed are presented in Table 5.

Table 5: Descriptive statistics of DBH collected from the field

Descriptive statistics	
Mean DBH (cm)	21.71
Standard deviation (cm)	12.97
Minimum (cm)	10
Maximum (cm)	90
Count	769

From the results of the descriptive statistics presented above, average tree DBH was 21.71cm, and the standard deviation was 12.97cm. This indicates that the tree DBH was 12.97cm dispersed from the mean. The minimum and maximum tree DBH were 10cm and 90cm respectively.

Graphical analysis was conducted to determine the occurrence of the tree DBH sampled in the field. The results are presented in the histogram.

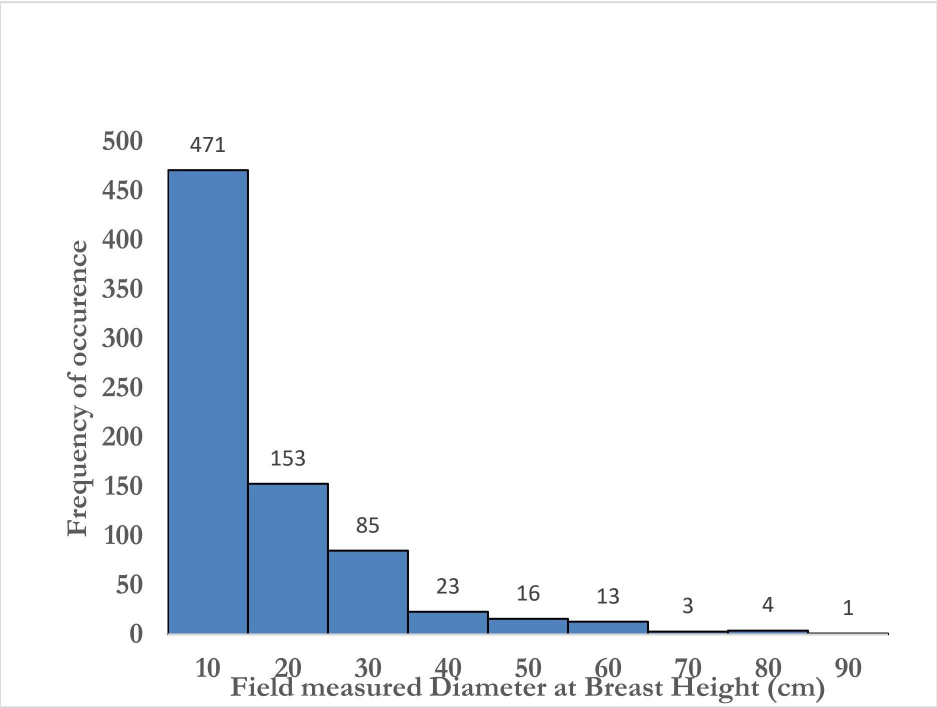

Figure 9: Distribution of field measured DBH

It can be seen from the histogram, that the positive skewness exhibited by the DBH. It may be attributed to the fact that only DBH equal or greater than 10cm were measured in the field. Also, maybe reflecting the age of the trees. Trees that possessed DBH between 10cm and 20cm were predominantly found in the study area, and the frequency of occurrence decreased with increase in age of the trees.

4.2. Tree crown delineation accuracy assessment

Object based image analysis was used to delineate tree crowns from the orthomosaic images. The delineation of the tree crowns served as the basis for extracting crown projection area (CPA) from the orthophoto. The CPA was required to model the relationship between field DBH. The accuracy was assessed by spatial join of the manually digitized (reference) polygons and automatic delineated tree crowns from the eCognition software. The validity of the segmentation was calculated by oversegmentation, under segmentation and D value as described in equations 1, 2 and 3 in the methodology section. The results of the analyses are presented in Table 6. Figure 10 shows an example of the segmented tree crowns.

Table 6: Segmentation error and accuracy for tree crown delineation

Study site	Segmentation error type		Fractional error	Accuracy(%)
1	Over segmentation	0.11	0.37	63
	Under segmentation	0.71		
2	Over segmentation	0.09	0.42	56
	Under segmentation	0.81		
3	Over segmentation	0.13	0.51	49
	Under segmentation	0.87		

From the accuracy of the delineated tree crowns, site 1 had higher accuracy of 63% and error of 37%. Site 2 had accuracy of 56% and error detected was 42%, while site 3 possessed an accuracy of 49% and error of 51%. The accuracy of the segmentation was relatively fair.

The results of segmentation accuracy assessment answered research question 1 relating to Object Based Image Analyses.

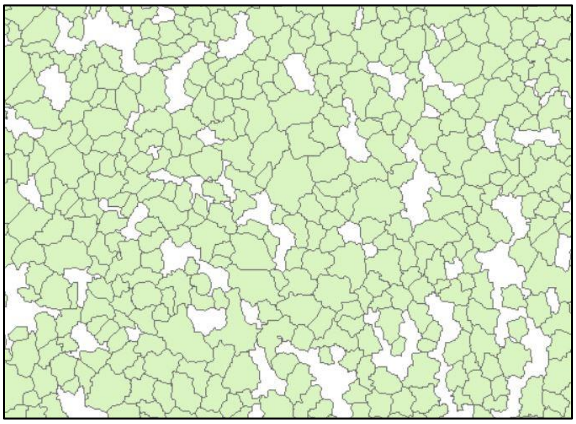

Figure 10: Snapshot of the segmented tree crowns

4.3. Accuracy assessment of the DTM in relation to the GNSS points

Validation of the DTM generated from LiDAR and UAV sourced data for the three sites were evaluated and compared to the GNSS points to ascertain their deviations from the line of fit. The was required to select the best CHM for the estimation of aboveground biomass and reduce the influence of errors in the modelled tree height on the estimated AGB values. The errors were computed using the root mean square error RMSE approach. The results are presented in the Table 7.

Table 7: DTM accuracy in relation to the GNSS points

	LiDAR sourced DTM RMSE (m)	UAV sourced DTM RMSE (m)
Site 1	2.90	0.20
Site 2	3.02	0.12
Site 3	26.10	3.70

From the results computed for the accuracies of the DTM, it can be seen that the ALS derived terrain model possessed higher RMSE values for all study sites. The UAV sourced terrain model had lower values for all sites, however errors in both terrain model increased in site 3. Based on the errors of the terrain models, the UAV derived terrain models were more accurate since they had lower RMSE values.
The DTM accuracy assessment answered research question 2 pertaining to Canopy Height Modelling

Afterwards, the canopy height models were generated from the subtraction of the DTM from the DSM for the 3 sites. The results are presented below

4.4. Canopy Height Modelling

A total of 6 Canopy Height Models were created for the three study sites. Two Canopy Height Models were created for each site, one derived from LiDAR and another from the UAV. For the ease of comparison, the created CHM are presented sequentially.

4.4.1. Canopy Height Model using LiDAR and UAV data for site 1

The CHMs were generated from the subtraction of the DTM from the DSM. The area is characterised by relatively undulating terrain and the forest canopy is relatively open as well. The created CHMs created are presented in Figure 11

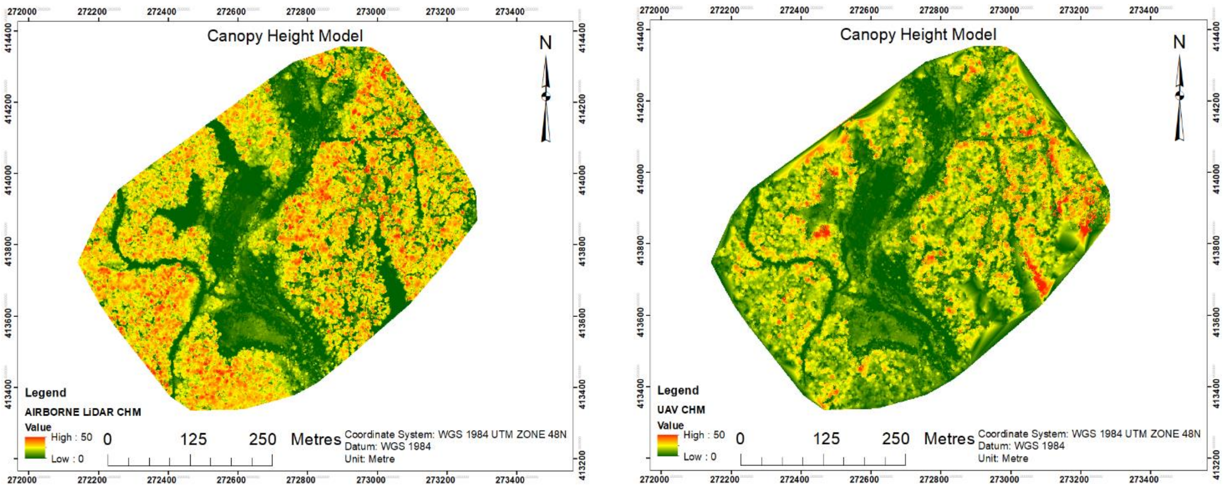

Figure 11: Canopy Height Models created using LiDAR and UAV data.

4.4.2. Canopy Height Model using LiDAR and UAV data for site 2

Similarly, the CHM was produced from the subtraction of the DTM from the DSM of the LiDAR and UAV. The area is characterised by flat terrain and open forest canopy. The UAV imagery captured extended out of the LiDAR data boundary. However, tree parameters were obtained in the area common to both data. So, only the CHM created using the UAV data is shown in Figure 12, and the image of overlap between both data are presented in appendix 2.

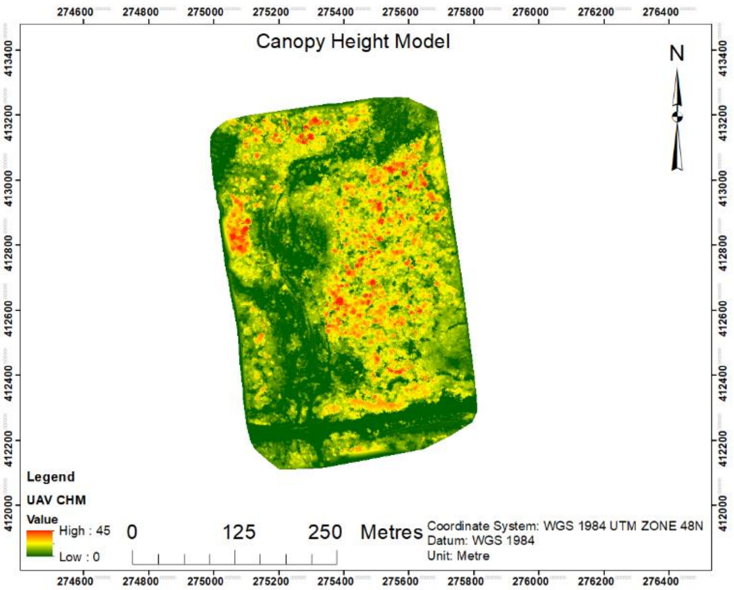

Figure 12: Canopy Height Model created using UAV data.

4.4.3. Canopy Height Model using LiDAR and UAV data for site 3

Same process described for the creation of CHM was also used to derived the CHM for site 3. The area is characterised by very undulating terrain and dense forest canopy The created CHMs are presented in Figure 13.

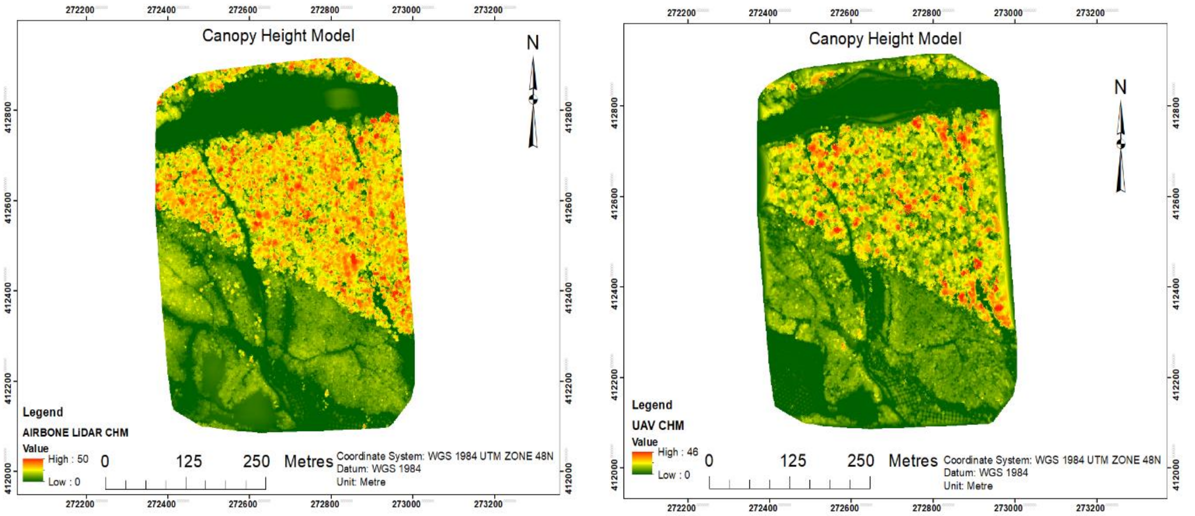

Figure 13: Canopy Height Models created using LiDAR and UAV data

After creation of the CHMs which served as input data for the tree height extraction and comparison. However, tree height was only extracted and compared for site 1 and 2. This was based on the errors obtained in the DTM accuracy in site 3. The RMSE values obtained in the terrain models were higher than the values obtained in sites 1 and 2. Also, because of vast differences in the RMSE values of the terrain models of both data, comparison of tree height of the tree height won't be reasonable. Thus, only the CHMs created for site 1 and 2 were used for further analyses. The results of the estimated forest tree height are presented in the following section.

4.5. Estimation of tree height and comparison using the LiDAR and UAV derived CHMs

Tree height was estimated using two methods; Airborne LiDAR and UAV derived CHMs. The tree height were compared using linear regression, Pearson's correlation, RMSE and t-test.

4.5.1. Tree height estimation and comparison for site 1

In total, 286 corresponding trees were retrieved from LiDAR and UAV CHMs. The results of the descriptive statistics for the modelled trees are presented in Table 8.

Table 8: Descriptive statistics of tree height estimated using LiDAR and UAV CHMs

	LiDAR estimated tree height (m)	UAV estimated tree height (m)
Mean	23.76	20.40
Standard deviation	6.93	5.44
Minimum	7.62	6.06

Maximum	39	32..74
Count	286	286

From the results of the descriptive statistics, it can be seen that the trees modelled from the LiDAR CHM were over 3m higher on average than the height of trees modelled from the UAV CHM. Also, the estimated trees from the LiDAR data had a higher standard deviation with a value of 6.93m, compared to the standard deviation of 5.44m recorded from the UAV CHM. This implies that LiDAR estimated trees are more dispersed from the mean than the trees estimated from the UAV CHM. The minimum tree height estimated from the LiDAR CHM is almost 2m higher, with a value of 7.62m than the minimum tree height estimated from the UAV CHM which had a value of 6.06m. Furthermore, the maximum tree height estimated from the LiDAR CHM is 7m higher than the maximum value obtained from the UAV CHM.

Line of best fit was conducted with a regression equation using the UAV data as the independent variable and LiDAR as the dependent variable presented with a scatter plot in Figure 14. The R^2 of 0.71, RMSE of ±3.38m and correlation coefficient of 0.84 was established. The regression summary statistics are presented in Table 9.

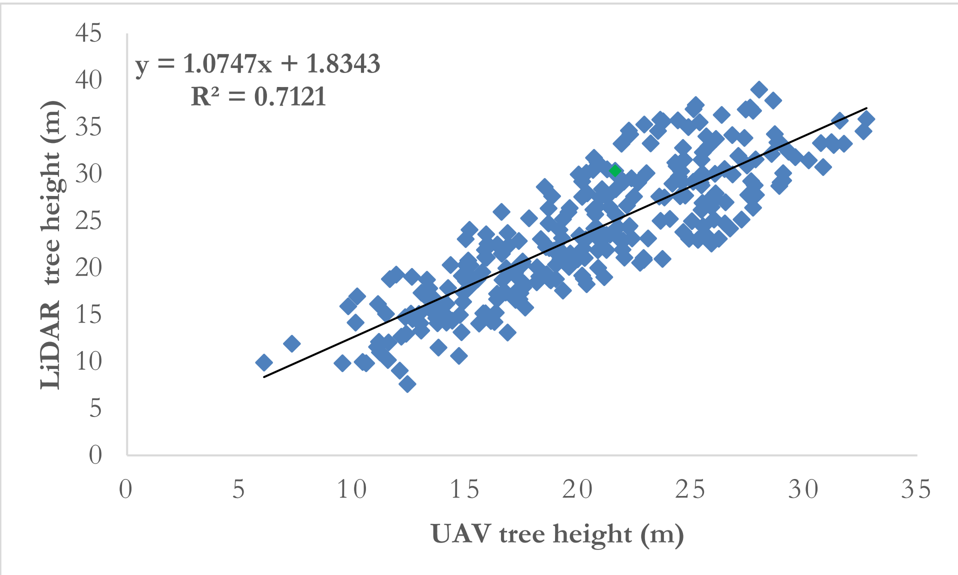

Figure 14: Scatter plot of the relationship between LiDAR and UAV estimated tree height

Table 9: Regression statistics for estimated trees froms LiDAR and UAV CHMs

Regression statistics	
Multiple R	0.84
R Square	0.71
Adjusted R Square	0.71
Standard Error (m)	3.72

RMSE (m)	3.38
Observations	286

Afterwards, an f-test was conducted to determine if the estimated trees from both data had an equal variance or not. The results are presented in Table 10.

Table 10: F-Test Two-Sample for Variances between estimated tree height from LiDAR and UAV CHMs

	ALS estimated tree height	UAV estimated tree height
Mean	23.76	20.40
Variance	48.05	29.62
Observations	286	286
df	582	506
F	1.21	
P(F<=f) one-tail	2.4636E-05	
F critical one tail	1.15	

The results of the f-test show that at α =0.05, there is an unequal variance between the estimated trees from both CHMs, p value is less than 0.05.

Based on the results of the f-test, a test assuming unequal variances was conducted to determine if there is a significant difference between tree height estimated from both CHMs. The results are presented in Table 11.

Table 11: t-Test Two-Sample Assuming Unequal Variances between estimated tree height from LiDAR and UAV CHMs

	ALS estimated tree height	UAV estimated tree height
Mean	23.76	20.40
Variance	48.05	29.62
Observations	286	286
Df	540	
Hypothesized Mean Difference	0	
t Stat	6.44	
P(T<=t) two-tail	2.5827E-10	
t Critical two-tail	1.96	

The results of the t-test show, at α =0.05, that there is a significant difference between tree height extracted from the CHMs, $p < 0.05$.

Similarly, tree height estimation and comparison were conducted for site 2, and the results are presented below.

4.5.2. Tree height estimation and comparison for site 2

In total, 262 corresponding trees were retrieved from both data. The results of the descriptive statistics conducted for the variables are shown in Table 12.

Table 12: Descriptive statistics of the estimated tree height from LiDAR and ALS CHMs

	LiDAR estimated tree height	UAV estimated tree height
Mean	19.93	19.05
Standard deviation	6.19	5.47
Minimum	5.03	6.06
Maximum	34.58	32.61
Count	262	262

From the results of summary statistics presented above, it can be seen, that on the average, the estimated trees from the LiDAR CHM were 0.88m higher than the average trees estimated from the UAV CHM. Also, trees estimated from the LiDAR CHM had a higher standard deviation value of 6.19m, than the standard deviation of trees recorded from the UAV CHM with a value of 5.47m. This implies that the trees retrieved from the LiDAR CHM were more spread from the mean than the trees estimated using UAV CHM

Subsequently, line of best fit was conducted with a regression equation and presented with a scatter plot in Figure 15. Coefficient of determination was (R^2) of 0.80, RMSE of ±0.88m and a correlation coefficient of 0.89 was established. The regression summary statistics are presented in Table 13.

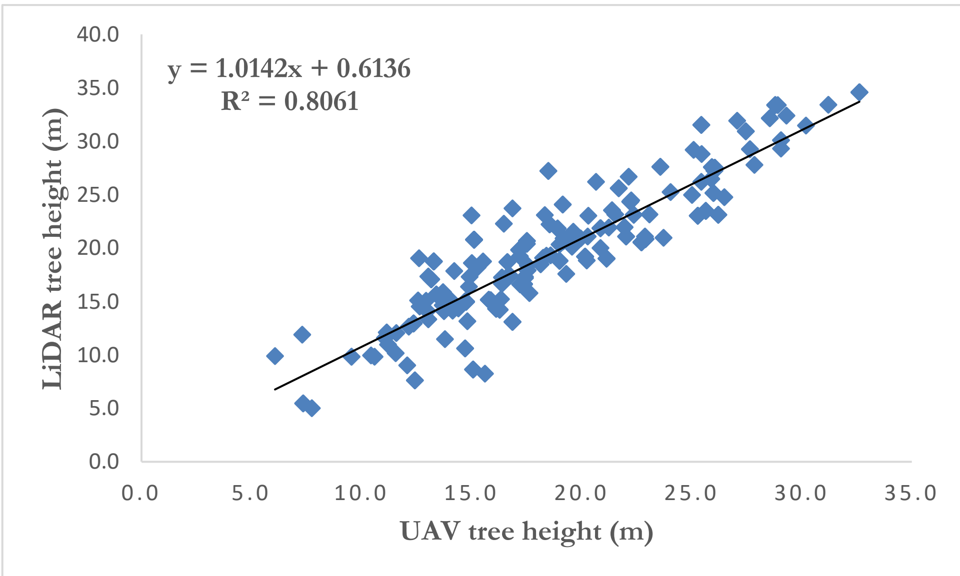

Figure 15: Scatter plot for the relationship between LiDAR and UAV estimated tree height

Table 13: Regression statistics between estimated tree height from LiDAR and UAV CHMs

Regression statistics	
Multiple R	0.89
R Square	0.80
Adjusted R Square	0.80
Standard Error (m)	2.73
RMSE (m)	0.88
Observations	262

Then, f-test was used to determine if the estimated tree height exhibited equal variance or not. The results are presented in Table 14.

Table 14: F-Test Two-Sample for Variances between estimated tree height from LiDAR and UAV CHMs

	ALS estimated tree height	UAV estimated tree height
Mean	19.93	19.05
Variance	38.32	30.02
Observations	262	262
Df	261	261
F	1.27	
P(F<=f) one-tail	0.02	
F Critical one-tail	1.22	

The results of the f-test show at α =0.05, there is an unequal variance between the estimated tree height from both data, p value <0.05.

Then, a t-test assuming unequal variance was conducted. The results are shown in Table 15.

Table 15: t-Test Two-Sample Assuming Unequal Variances between estimated tree height from ALS and UAV CHMs

	LiDAR estimated tree height	UAV estimated tree height
Mean	19.93	19.05
Variance	38.32	30.02
Observations	262	262
Df	522	
Hypothesized Mean Difference	0	
t Stat	1.73	
P(T<=t) two-tail	0.08	
t Critical two-tail	1.96	

The results of the t-test show that at α =0.05, there is no significant difference between tree height estimated from both CHM, p value >0.05.

The results of tree height estimation and comparison presented above answered research question 3 about the canopy height modelling.

4.6. Modelling the relationship between crown projection area and Diameter at Breast Height (DBH)

To model the relationship between CPA and DBH, tree crowns were manually segmented on the orthophoto using visual image interpretation. The use of predicted DBH from CPA to model AGB is biased due to errors in the segmented CPA. Therefore to reduce the error introduced into the AGB values, the manually digitised tree crowns were used. CPA of trees that had one to one match with the DBH were used for model development and validation. The results are presented below.

4.6.1. Model development for site 1

Simple linear, logarithmic, power and quadratic models were developed to ascertain how accurately DBH can be predicted from CPA. The modelling of the relationship between CPA and DBH was done with 74 trees. The randomly divided 60% (44 trees) of the dataset were used to develop the models. The models were compared using the RMSE and coefficient of determination. The results of the developed models are shown in Table 16 and Figure 16.

Table 16: Models developed for prediction of DBH

Model	Equation	R^2	RMSE
Linear	DBH(cm)=0.7922*CPA+13.535	0.74	6.83
Logarithmic	DBH(cm)=18.404*ln(CPA)-21.466	0.65	9.12
Power	DBH(cm)=5.681*(CPA^0.544)	0.59	7.51
Quadratic	DBH(cm)=0.0023*CPA^2+0.6383*CPA+15.181	0.74	6.60

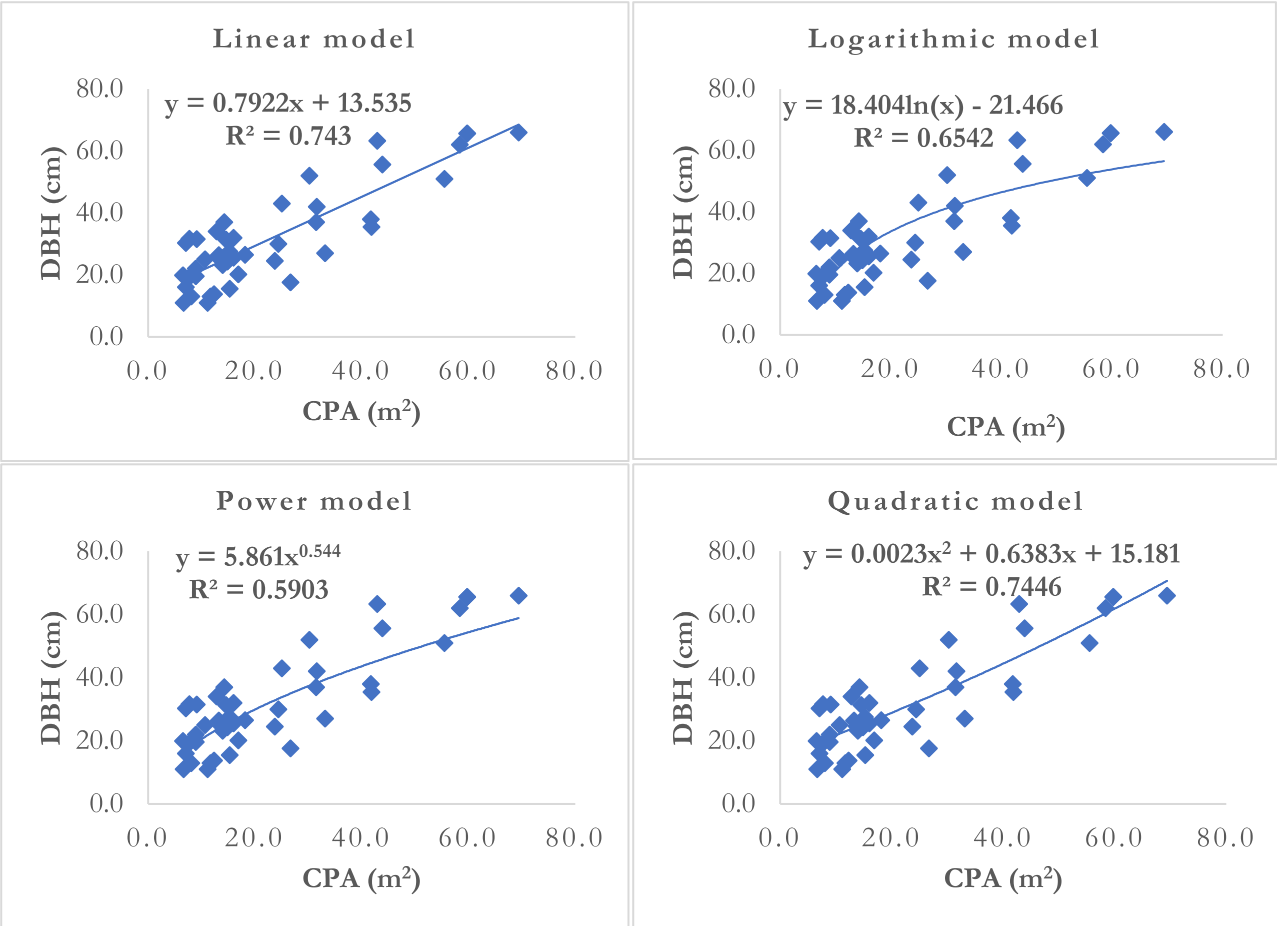

Figure 16: Models developed for prediction of DBH

From the results of the model developed and compared, The linear and quadratic models had the highest predictive power and least errors compared to power and logarithmic. However, quadratic model was selected for the DBH prediction based on it lowest RMSE values.

A one way analysis of variance (ANOVA) was employed to test the significance of the quadratic model, and the results in Table 17 which show that regression was statistically significant at 95% confidence level.

Table 17: ANOVA test results for the quadratic model

ANOVA test for significance					
	df	SS	MS	F	Significance F
Regression	1	4280.944	4280.944	99.42981	1.03E-10
Residual	28	1205.538	43.05493		
Total	29	5486.482			

4.6.2. Model validation

The predicted DBH values from the quadratic model were plotted against the observed DBH. The model was validated using randomly selected 40% (30 trees) of the dataset. The results show a coefficient of determination R^2 of 0.78 (Figure 17). This means that 78% of DBH measured in the field was explained by the quadratic model. The test of goodness of fit was done using RMSE which resulted in 6.33cm.

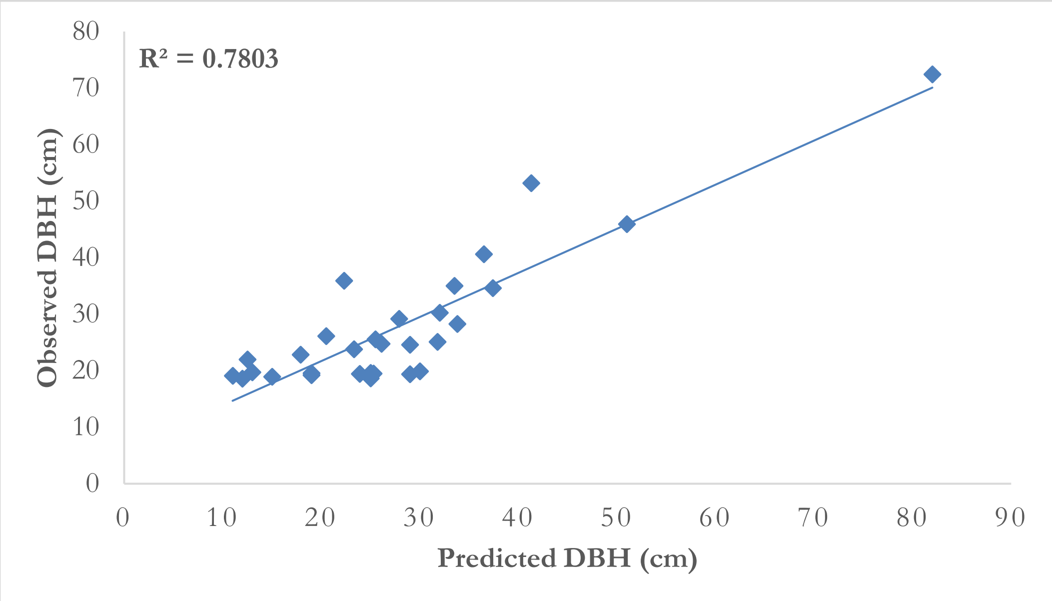

Figure 17: Scatter plot for model validation

4.6.3. Model development for site 2

Similarly, simple linear, logarithmic, power and quadratic models were developed and compared for the relationship between CPA and DBH. The modelling of the relationship between CPA and DBH was done with 30trees. The randomly divided 60% dataset were used to develop the models for DBH prediction. The models were compared using the coefficient of determination (R^2) and RMSE. The results are presented in Table 18 and Figure 18.

Table 18: Models developed for prediction of DBH

Model	Equation	R^2	RMSE
Linear	DBH(cm)=3.4024*CPA+7.2668	0.82	10.65
Logarithmic	DBH(cm)=21.008*ln(CPA)-5.0272	0.57	13.53
Power	DBH(cm)=10.248*(CPA^0.5434)	0.52	11.03
Quadratic	DBH(cm)=-0.0993*CPA^2+1.1284*CPA+14.832	0.86	9.49

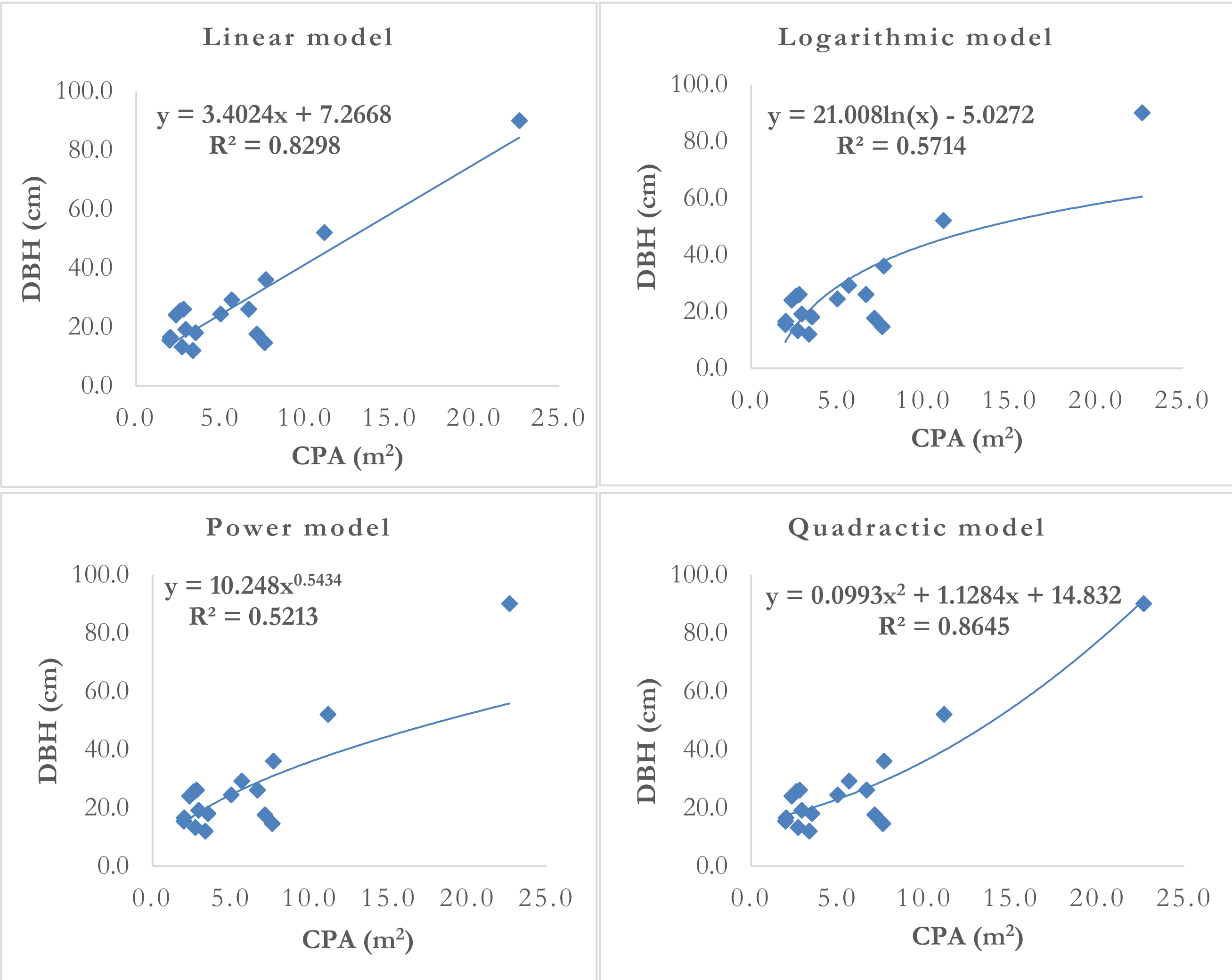

Figure 18: Models developed for prediction of DBH

From the results presented in Figure 18 and Table 18, it can be seen that the linear and quadratic models had the highest predictive power. However, quadratic model was selected for the prediction of DBH based on the lowest RMSE values. The data point of a tree measured in the field with a very large DBH and CPA was far from other points and somehow influences the models as seen on the scatter plots. But could not be removed because of limited sample size.

A one way analysis of variance (ANOVA) was employed to test the significance of the quadratic model, and the results in Table 23 which show that regression was statistically significant at 95% confidence level.

Table 19: ANOVA test for the quadratic model

ANOVA test for significance					
	df	SS	MS	F	Significance F
Regression	1	2047.591	2047.591	50.28069	3.33E-05
Residual	10	407.232	40.7232		

Total	11	2454.823

4.6.4. Model validation

The predicted DBH values from the quadratic model were plotted against the observed DBH. The model was validated using randomly selected 40% of the evaluation dataset. The results show a coefficient of determination R^2 of 0.83 shown in the scatter plot in Figure 19. This means that 83% of DBH measured in the field was explained by the quadratic model. The test of goodness of fit was done using RMSE which resulted in 5.82cm.

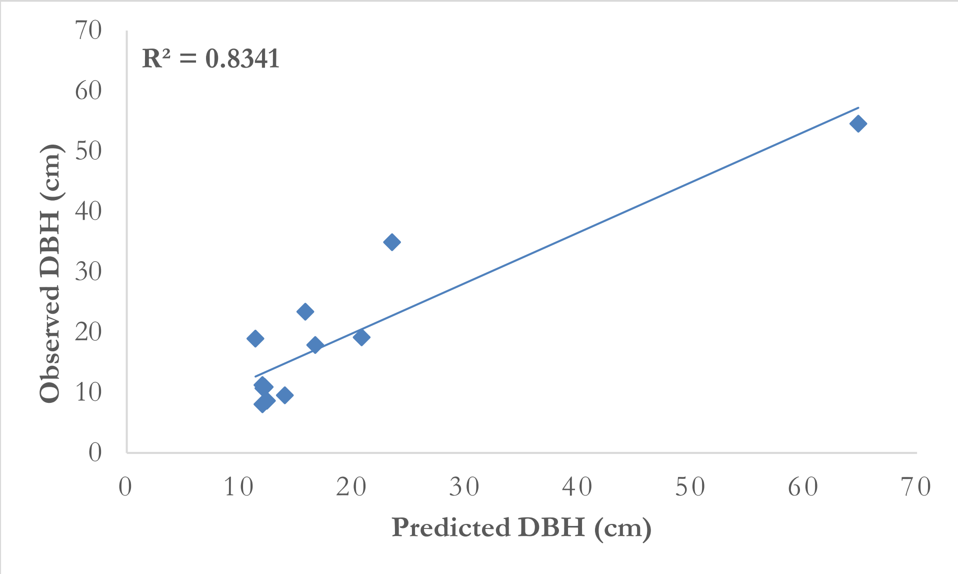

Figure 19: Scatter plot of model validation

The results presented above answered research question 1 relating to the modelling the relationship between CPA and DBH.

4.7. Aboveground biomass and carbon estimation

The tree height estimated from the UAV CHM was used to model AGB. It was found to be more accurate in the modelling of forest tree height, because of less errors in the DTM. This was required to reduce the errors from the modelled tree height for the estimation of AGB

The estimation of AGB was done using two methods; field measured DBH and estimated tree height, and predicted DBH from the quadratic model and estimated tree height. Allometric equation used for the estimation of AGB was adopted after (Chave et al., 2014), which is applicable to tropical rainforest. Afterwards, carbon stock was obtained from the estimated AGB using a conversion factor of 0.47. The AGB estimated using field measured DBH was compared to AGB estimated using predicted DBH. The results are presented in the following subsections.

4.7.1. Aboveground biomass and carbon estimation for site 1

The AGB was estimated with 74 trees that were used for model development and validation. The trees had one to one match between the CPA, DBH and estimated tree height. A total of 52396.8kg and 24628.5kg of AGB and carbon was estimated in the study area using the first method (field DBH and estimated tree height). Total of 708kg/tree of AGB was obtained.

Also, 52991.6kg and 24906.1kg of AGB and carbon was estimated using the second method (predicted DBH and estimated tree height).

4.7.2. Aboveground biomass carbon estimation for study site 2

Similarly, AGB was estimated with 30 trees the estimated AGB and carbon stock using method one was 17207.4kg and 8087.5kg. Therefore 573kg/tree of AGB was obtained.

While the estimated AGB and carbon using the second method was 9548.3kg and 4487.7kg respectively.

The modelling of AGB answered objective 1 relating to the allometric modelling of AGB.

To determine if there is a significant difference in the AGB estimated using both methods, f-test and t-test were conducted. The results are presented in Tables 20, 21, 22 and 23.

Table 20: F-test Two-Sample for Variances between AGB estimated using field DBH and predicted DBH

	AGB estimated using field DBH (kg)	AGB estimated using predicted DBH (kg)
Mean	708.06	716.10
Variance	539875.1	511589.1
Observations	74	74
df	73	73
F	1.05	
P(F<=f) one-tail	0.40	
F critical one tail	1.47	

The results of the f-test presented in Table 20 show, that they had equal variance, $p > 0.05$. Thus, t-test assuming equal variances was used for determining significant difference.

A T-test assuming equal variance was used to establish if there is a significant difference between estimated AGB using field measured and predicted DBH or not. The results are presented below.

Table 21: T-test Two-Sample assuming equal Variances between AGB estimated using field DBH and predicted DBH

	AGB estimated using field DBH (kg)	AGB estimated using predicted DBH(kg)
Mean	708.06	716.10
Variance	539875.1	511589.1
Observations	74	74
Df	146	146

Hypothesized Mean Difference	0
t Stat	-0.06
P(T<=t) two-tail	0.94
t Critical two-tail	1.97

The results of the t-test show that there is no significant difference between the estimated AGB using the two methods, p value > 0.05. Afterwards, t-test was used to determine the difference between AGB estimated using field and predicted DBH in combination with the UAV estimated tree height for site 2, and the results are shown below.

Table 22: F-test Two-Sample for Variances between AGB estimated using field DBH and predicted DBH

	AGB estimated using field DBH (kg)	AGB estimated using predicted DBH (kg)
Mean	573.57	318.27
Variance	1488531	68314.56
Observations	30	30
df	29	29
F	21.78	
P(F<=f) one-tail	4.61E-13	
F critical one tail	1.86	

The results of the f-test show that they had unequal variance, p <0.05. Thus, t-test assuming unequal variances was used for determining significant difference. The results are shown below

Table 23: T-test Two-Sample assuming unequal Variances between AGB estimated using field DBH and predicted DBH

	AGB estimated using field DBH (kg)	AGB estimated using predicted DBH(kg)
Mean	537.57	318.27
Variance	1488531	68314.56
Observations	30	30
Df	32	
Hypothesized Mean Difference	0	
t Stat	1.12	
P(T<=t) two-tail	0.27	
t Critical two-tail	2.03	

The results of the t-test revealed that there is no significant difference between the estimated AGB using the two methods namely, field measured and predicted DBH and in combination with the tree height retrieved from UAV CHM, p value > 0.05.

Comparison of both methods for the estimation of AGB answered research question 1 relating to allometric modelling of AGB within the study area.

5. DISCUSSION

5.1. Segmentation accuracy

Previous studies have shown that the accuracy of the tree crown segmentation depends on a lot of factors; noise, spatial and spectral as well as the optimal parameters setting employed during the image segmentation process (Möller et al., 2009).

In multiresolution segmentation, the size and homogeneity of resultant image objects is determined by the scale parameter (Drăguţ, et al., 2010). Of which getting an optimum scale parameter is reliant on trial and error approach.

Also, the validation of segmentation is based on one to one match between the polygons of the automatic and manual segments as well as their position in space (Clinton et al., 2010). Positional error of the GPS in matching the trees observed in the field to the image also occurred see Figure 20. This result in the differences in the area, shape and boundaries of the polygons derived from manual and automatic segments as mentioned by (Zhan, Molenaar, Tempfli, & Shi, 2007).

Furthermore, using multiresolution, the scale factor changes as a result of different sizes of object, and shape and compactness vary because of the different properties of objects belonging to different classes (Mesner & Oštir, 2014). This occurred as the forest had different species composition and of different ages. Therefore the size of the object had an influence on the segmentation output. The influence of positional error, trees composition on segmentation accuracy is shown in Figure 20.

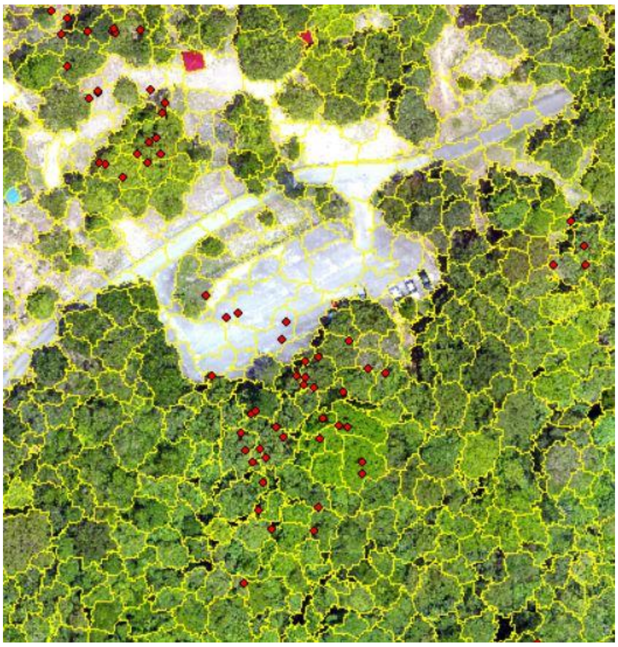

Figure 20: Effects of positional error of the GPS and forest structure on segmentation output

The red dots represent the GPS points taken at the tree base.

5.2. Accuracy assessment of Digital Terrain Model

Previous studies demonstrated that LiDAR data are more accurate for the generation of elevation models for the vertical characterization of forest structure (Huang et al., 2009; Wallace et al., 2016). However, the results of this study showed that the DTM generated using UAV sourced data was better than the one based on airborne LiDAR data.

It was found that differences exist in the point density of both datasets. The LiDAR data had 5point/m^2, compared to the point density of UAV datasets which have 27.39point/m^2, 13.83/m^2 and 26.3m^2 for the three study sites/blocks. This higher point density of the UAV data could have caused its better this superior than the LiDAR data. This is in agreement with the study done by Okojie, (2017), who found UAV sourced DTM to be more accurate than the DTM derived from ALS data. Same results was also found by (Thiel & Schmullius, 2017).

The derivation of elevation model is based on interpolation that enables the prediction of unknown values based on known values (Debella-Gilo, 2016). Also, the study done by Simpson, et al., (2017) found that the creation of an accurate and well-detailed surface model is dependent on the number of points and the relative distance between the point. The LiDAR data had sparse point cloud for interpolation, this could have affected its ability to perform and produce accurate surface models, compared to the UAV that had higher number of points (Thiel & Schmullius, 2017).

In addition to the point density, previous studies found that the forest structure and terrain also affect the accuracy of DTM generation in a forest ecosystem (Estornell, et al., 2011; H. Hyyppä et al., 2005; J. Hyyppä et al., 2008). This study was conducted across three sites, each site had distinct forest structure and topograpgy. Though the LiDAR and UAV data performed well in sites 1 and 2, this could be due to relatively open forest canopies and less undulating terrain. Thus, the point was able to penetrate to the forest floor in combination with the relatively flat terrain. Nevertheless, the UAV showed better performance than th LiDAR, because of its higher point density with more chance of hitting a tree top and the forest floor.

However, site 3 is a complex forest stand, with higher forest canopy density and undulating terrain and here the results is less accurate. This is in agreement with the study done by (Salleh, Ismail, & Rahman, 2015), where the study found a statistically significant relationship between the accuracy of modelling forest floor with forest canopy cover and the terrain.

In addition, Balenović et al., (2016), found that the accuracy of a DTM generated using UAV photogrammetry varies across different land cover classes. They assessed the quality of a DTM across three land cover classes; forests, shrubs and grassland. They observed that the DTM accuracy is dependent on the complexity of the landcover type as the least accurate DTM was found in the forest landcover class.

Furthermore, Debella-Gilo & Iii, (2016) found the relation between the DTM accuracy with varying topographic and ground cover characteristics. The study was conducted across four study sites.

- Site 1 was a bare area with gradual slope
- Site 2 was steep area covered partly dense vegetation

- Site 3 was built up area with flat terrain
- Site 4 was a complex topograpgy with steep and undulating terrain.

Therefore, in a closed forest canopy, there was a reduction in the number of point to reach the forest floor, and in combination with the increase in the slope angle caused by the undulating terrain. Based on this findings, the forest structure and terrain could have affected the accuracy of the DTM obtained in site 3. 3D photogrammetry using stereo images obtained from UAV platform, has the potential to produce better accuracy in the interpolation of DTM when the optimum flight height, percentage of front and side of overlap are used in capturing the stereo imagery.

5.3. Comparison between tree height estimated using LiDAR and UAV CHM

In site 1, the mean tree height difference between the extracted tree height from the UAV and ALS CHM was 3.36m, and the root mean square error of the LiDAR estimated tree height was found to be 3.38m. This means that there was an overestimation of tree height from the LiDAR data. The overestimation was caused by the error in the DTM that propagated into the estimated tree height. The t-test conducted revealed that there is a significant difference between the tree height derived from ALS and 3D photogrammetry from UAV data ($p < 0.05$). This significant difference was caused by the overestimation of tree height from the errors in DTM. Not all trees have been hit by the laser pulse due to the sparsity of points

The root mean square error of 0.88m and mean difference of 0.88m was found between tree height extracted using airborne LiDAR and UAV for site 2. The t-test revealed there was no significant difference between the extracted tree height based on UAV and ALS CHM ($p > 0.05$). This could be true since the mean tree height difference between both data was 0.88m and the RMSE deviation from the line of fit was also 0.88m. However, it is relevant to be aware of the error found in the LiDAR data as this could influence the AGB values from the errors in the modelled tree height. Nevertheless, there was a positive correlation between the the comparison of tree height modelled using LiDAR and UAV 3D point cloud for both sites/blocks. This correspond with the results of previous studies. The study conducted by Wallace, et al., (2016) found a positive correlation between the estimated tree height from aerial photo 3D UAV point cloud and LiDAR. Also, Vastaranta et al., (2013) found positive correlation when tree height measurements by LiDAR system was compared with the tree height measured by 3D photogrammetry of UAV images.

5.4. Relationship between Crown projection area and field measured Diameter at Breast Height

The relationship between Diameter at Breast Height and crown projection area was found to be positive and significant. Four models were compared and the quadratic model was chosen because of its high predictive power and least error. This contradicts the results of the Kumar, (2011), who found a linear relationship existing between CPA and DBH in a tropical forest. Which implies that when a tree grows, the CPA does same. The results obtained in this study is similar to the findings of Baral, (2011), who stated that a nonlinear relationship exist between CPA and DBH in a tropical rainforest. Also, Hemery, Savill, &

Pryor, (2005), found that linear relationship cannot not be found between DBH and CPA, where the trees possessed DBH larger than 40cm in a dense forest ecosystem. This is true, since the trees sampled had DBH larger than 40cm.

Similarly, Shimano, (1997), obtained nonlinear relationship between CPA and DBH. This is because in a dense forest with canopy closure, there is competition between the trees for sunlight. Thus, the rate of growth of the CPA is slow down because of the competition of neighbouring crowns. However, the DBH continues to increase, though at a slower rate and the CPA will start stabilizing and becomes constant when the DBH has grown sufficiently (Shimano, 1997).

The model was developed with few sample size and this reduces it statistical power. Despite that, it was able to establish positive relationship between CPA and field measured DBH using orthophoto as input data. Upscaling segmentation accuracy can help increase the statistical power by using the automatic segmented tree crowns to develop the model and apply it to the entire study area.

5.5. Estimation of aboveground biomass

The estimated aboveground biomass was calculated using the allometric equation developed by (Chave et al., 2014) which is applicable to the tropical rainforest, and the model incorporates tree height, Diameter at Breast Height, and wood density. The method used in this study is comparable to the method used by Mtui, (2017). The study used UAV data to model tree height, and subsequently estimate AGB and carbon stock, in the tropical rainforest of Malaysia. Although both methods were similar, the method used in this study was found to be better than the method he employed in his study. This is because his method did not evaluate the accuracy of the CHM used in the estimation of AGB. Therefore, uncertainty in the error of the CHM that was introduced into the AGB values from the modelled tree height was unknown in his method. The comparison of the difference in estimated AGB using t-test revealed that there was no significant difference using the field measured and predicted DBH (p value > 0.05). However, using predicted DBH to model AGB/carbon had errors introduced into the AGB values from the model used. The difference in the amount of AGB values obtained resulted from the errors in the models. Also the sample same size used for the estimation of AGB also affected the statistical power.

5.6. Sources of errors

According to Petrokofsky et al., (2012) errors in aboveground biomass estimation can be introduced in many ways such as the use of wrong allometric equation, inaccurate measurement of variables, instruments and calibration errors.

Tree height and Diameter at Breast Height are the two most common variables used for estimation of AGB. It is relevant to enumerate the likely sources of error in this study.

The first potential source of was the GPS. The trees position and centre of sample plots were recorded using an iPAQ. The iPAQ had an accuracy between 2-4 metres. Some data points were clustered on one a tree crown, while some were far away from the plots (Figure 21). This may have caused mismatch and shift in the position of the trees during matching of trees from remotely sensed data and the trees measured in the field.

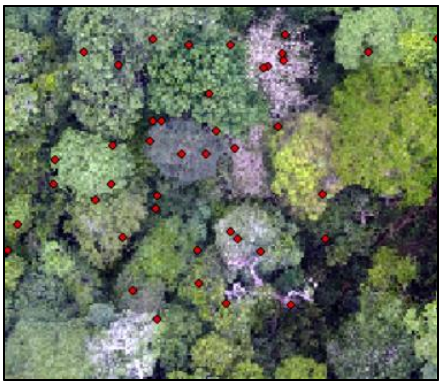

Figure 21: Positional shift and mismatch caused by errors in the GPS

The red dots indicate the GPS points taken at the tree base.

Another source of error was the Canopy Height Model used for the estimation of tree height.

The DTM used for the tree height estimation had an RMSE of 0.20m and 0.12m for site 1 and 2. The tree height was overestimated by 0.20m and 0.12m and these errors has influenced the estimated AGB values. Therefore, the errors in the estimated tree height may have led to an under or over-estimation of biomass and carbon values.

A third potential source of error was the allometric equation used for the estimation of biomass. The non-site species-specific allometric equation developed by (Chave et al., 2014) was used for the estimation of AGB. The equation does not incorporate species, age, topography, soil and climatic conditions (Basuki, et al., 2009).

Furthermore, the LiDAR data was acquired in November 2014, while the UAV datasets were acquired in September and October 2017. The height of the trees may have slightly increased because of the continuos growing season in between the two periods.

6. CONCLUSION AND RECOMMENDATIONS

6.1. CONCLUSION

This study evaluated the performance of imagery captured with Unmanned Aerial Vehicle (UAV), to retrieve forest parameters and assessment of aboveground biomass in a tropical rainforest. According to the research questions and objectives, the following conclusions were made.

6.1.1. What is the accuracy of the tree crown segmentation?

The accuracy of tree segmentation was 63%, 53% and 49% respectively for the three sites.

6.1.2. What is the accuracy of UAV and airborne LiDAR data derived Digital Terrain Model?

The DTM generated by 3D photogrammetry using images acquired by the UAV was more accurate than the DTM based on the airborne LiDAR system.

6.1.3. Is there a significant difference between tree height *estimated* using airborne LiDAR and UAV?

There was a significant difference between estimated tree height using LiDAR and UAV 3D photogrammetry, $\alpha=0.05$, p value less than 0.05. The null hypothesis was rejected and alternate hypothesis accepted in site 1.
In site 2, there was no significant difference between estimated tree height using LiDAR and UAV CHM $\alpha=0.05$, p value greater than 0.05. The null hypothesis was accepted.

6.1.4. Is there a significant relationship between crown projection area and Diameter at Breast Height (DBH)?

There was a significant relationship between tree crown projection area and Diameter at Breast Height (DBH) $\alpha=0.05$, p value less than 0.05. The null hypothesis was rejected and the alternate hypothesis was accepted.

6.1.5. Is there a significant difference between AGB *estimated* using field measured DBH and predicted DBH?

There was no significant difference between AGB estimated using field measured and predicted DBH at $\alpha=0.05$, p value greater than 0.05. The null hypothesis was accepted. This statement hold true for the two sites.

6.2. Recommendation

- The modelling of forest tree height using UAV stand-alone datasets is recommended. This study has proven that DTM created exclusively using UAV data to perform better than the one based on airborne LiDAR. This is primarily due to its robust high point cloud for accurate interpolation of the surface models.

- It was discovered that increase in forest coverage limits the number of point to penetrate to the forest floor. Subsequent use of LiDAR data with higher point density and optimisation of the highest point density generation option in the photogrammetry processing software is required against the medium that was employed in this study is recommended. The choice of any of the data is a function of cost, availability, and the computational time for the photogrammetry processing. Also, information on the terrain is highly recommended since it also affected the accuracy of modelling forest tree height.
- Subsequently, Differential GPS should be used to record location of trees for better matching of tree parameters measured in the field and on the images.

LIST OF REFERENCES

Andersen, H.-E., Reutebuch, S. E., & Mcgaughey, R. J. (2006). A rigorous assessment of tree height measurements obtained using airborne lidar and conventional field methods. *Can. J. Remote Sensing*, *32*(5), 355–366. Retrieved from http://citeseerx.ist.psu.edu/viewdoc/download?doi=10.1.1.524.6362&rep=rep1&type=pdf

Andersen, H., McGaughey, R. J., Carson, W. W., Reutebuch, S. E., Mercer, B., & Allan, J. (2003). A comparison of forest canopy models derived from LIDAR and INSAR data in a Pacific Northwest conifer forest. *ISPRS Archives*, *34*(Part 3/W13), 211–217. Retrieved from http://www.treesearch.fs.fed.us/pubs/7347%5Cnhttp://www.isprs.org/proceedings/XXXIV/3-W13/papers/Andersen_ALSDD2003.pdf

Anderson, K., & Gaston, K. J. (2013). Lightweight unmanned aerial vehicles will revolutionize spatial ecology. *Frontiers in Ecology and the Environment*, *11*(3), 138–146. https://doi.org/10.1890/120150

Balenović, I., Marjanović, H., Vuletić, D., Paladinić, E., Sever, M. Z. O., & Indir, K. (2016). Quality assessment of high density digital surface model over different land cover classes. *Periodicum Biologorum*, *117*(4), 459–470. https://doi.org/10.18054/pb.2015.117.4.3452

Baral, S. (2011). *Mapping Carbon Stock Using High Resolution Satellite Images In Sub-Tropical Forest Of Nepal. ITC thesis. Enschede,The Netherlands*. Unpublished Masters Thesis, University of Twente, Enschede, The Netherlands. Retrieved from http://www.itc.nl/Pub/Home/library/Academic_output/AcademicOutput.html?p=11&y=11&l=20

Barnes, C., Balzter, H., Barrett, K., Eddy, J., Milner, S., & Suárez, J. C. (2017). Individual tree crown delineation from airborne laser scanning for diseased larch forest stands. *Remote Sensing*, *9*(3), 1–20. https://doi.org/10.3390/rs9030231

Basuki, T. M., Van Laake, P. E., Skidmore, A. K., & Hussin, Y. A. (2009). Allometric equations for estimating the above-ground biomass in tropical lowland Dipterocarp forests. *Forest Ecology and Management*, *257*(8), 1684–1694. https://doi.org/10.1016/j.foreco.2009.01.027

Bendig, J., Yu, K., Aasen, H., Bolten, A., Bennertz, S., Broscheit, J., … Bareth, G. (2015). Combining UAV-based plant height from crop surface models, visible, and near infrared vegetation indices for biomass monitoring in barley. *International Journal of Applied Earth Observation and Geoinformation International Journal of Applied Earth*, *39*, 79–87. https://doi.org/10.1016/j.jag.2015.02.012

Bing, D., Rajpar, M., & Zakaria, M. (2013). Avian Richness and Habitat Characteristics In Primary and Logged Hill Dipterocarp Tropical Rainforest Of Peninsular Malaysia. *Malaysian Nature Journal*, *65*(4), 300–316.

Brown, S. (2002). Measuring carbon in forests: Current status and future challenges. *Environmental Pollution*, *116*(3), 363–372. https://doi.org/10.1016/S0269-7491(01)00212-3

Calders, K., Newnham, G., Burt, A., Murphy, S., Raumonen, P., Herold, M., … Kaasalainen, M. (2015). Nondestructive estimates of above-ground biomass using terrestrial laser scanning. *Methods in Ecology and Evolution*, *6*(2), 198–208. https://doi.org/10.1111/2041-210X.12301

Cao, L., Coops, N. C., Innes, J. L., Sheppard, S. R. J., Fu, L., Ruan, H., & She, G. (2016). Estimation of forest biomass dynamics in subtropical forests using multi-temporal airborne LiDAR data. *Remote Sensing of Environment*, *178*, 158–171. https://doi.org/10.1016/j.rse.2016.03.012

Carreiras, J., Melo, J., & Vasconcelos, M. (2013). Estimating the Above-Ground Biomass in Miombo Savanna Woodlands (Mozambique, East Africa) Using L-Band Synthetic Aperture Radar Data. *Remote Sensing*, *5*(4), 1524–1548. https://doi.org/10.3390/rs5041524

Chai, T., & Draxler, R. R. (2014). Root mean square error (RMSE) or mean absolute error (MAE)? – Arguments against avoiding RMSE in the literature. *Geosci. Model Dev*, *7*, 1247–1250. https://doi.org/10.5194/gmd-7-1247-2014

Chave, J. (2005). Tree height measurement protocol – J Chave Measuring tree height for tropical forest trees A field manual for the CTFS sites. Retrieved July 28, 2017, from http://chave.ups-tlse.fr/chave/tree-height-protocol.pdf

Chave, J., Réjou-Méchain, M., Búrquez, A., Chidumayo, E., Colgan, M. S., Delitti, W. B. C., … Vieilledent, G. (2014). Improved allometric models to estimate the aboveground biomass of tropical trees. *Global Change Biology*, *20*(10), 3177–3190. https://doi.org/10.1111/gcb.12629

Clinton, N., Holt, A., Scarborough, J., Yan, L., & Gong, P. (2010). Accuracy Assessment Measures for Object-based Image Segmentation Goodness. *Photogrammetric Engineering and Remote Sensing*, *76*(3),

289–299. https://doi.org/10.14358/PERS.76.3.289
Dandois, J. P., Olano, M., & Ellis, E. C. (2015). Optimal altitude, overlap, and weather conditions for computer vision uav estimates of forest structure. *Remote Sensing*, *7*(10), 13895–13920. https://doi.org/10.3390/rs71013895
Debella-Gilo, M. (2016). Bare-earth extraction and dtm generation from photogrammetric point clouds with a partial use of an existing lower resolution dtm. *International Archives of the Photogrammetry, Remote Sensing and Spatial Information Sciences - ISPRS Archives*, *41*(B3), 201–206. https://doi.org/10.5194/isprsarchives-XLI-B3-201-2016
Derivaux, S., Forestier, G., Derivaux, S., Forestier, G., Wemmert, C., & Le Evre, S. (2010). Supervised image segmentation using watershed transform, fuzzy classification and evolutionary computation. *Pattern Recognition Letters*, *31*(15), 2364–2374. https://doi.org/10.1016/j.patrec.2010.07.007>
Drăguţ, L., Tiede, D., & Levick, S. R. (2010). ESP: a tool to estimate scale parameter for multiresolution image segmentation of remotely sensed data. *International Journal of Geographical Information Science*, *24*(6), 859–871. https://doi.org/10.1080/13658810903174803
Dubayah, R. O., Sheldon, S. L., Clark, D. B., Hofton, M. A., Blair, J. B., Hurtt, G. C., & Chazdon, R. L. (2010). Estimation of tropical forest height and biomass dynamics using lidar remote sensing at La Selva, Costa Rica. *Journal of Geophysical Research: Biogeosciences*, *115*(G2). https://doi.org/10.1029/2009JG000933
Edson, C., & Wing, M. G. (2011). Airborne Light Detection and Ranging (LiDAR) for Individual Tree Stem Location, Height, and Biomass Measurements. *Remote Sensing*, *3*(12), 2494–2528. https://doi.org/10.3390/rs3112494
Estornell, J., Ruiz, L. A., Velázquez-Martí, B., & Hermosilla, T. (2011). Analysis of the factors affecting LiDAR DTM accuracy in a steep shrub area, *4*(6), 521–538. https://doi.org/10.1080/17538947.2010.533201
Fan, J., Zeng, G., Body, M., & Hacid, M. S. (2005). Seeded region growing: An extensive and comparative study. *Pattern Recognition Letters*, *26*(8), 1139–1156. https://doi.org/10.1016/j.patrec.2004.10.010
Francisco Agüera-Vega, Fernando Carvajal-Ramírez, & Patricio Martínez-Carricondo. (2017). Assessment of photogrammetric mapping accuracy based on variation ground control points number using unmanned aerial vehicle. *Measurement*, *98*, 221–227. https://doi.org/10.1016/J.MEASUREMENT.2016.12.002
Gallay, M. (2013). Direct Acquisition of Data: Airborne laser scanning. *Geomorphological Techniques (Online Edition)*, *4*(1998), 16. Retrieved from http://www.geomorphology.org.uk/assets/publications/subsections/pdfs/OnsitePublicationSubsection/10/2.1.4_lidar.pdf
Gatziolis, D., Lienard, J. F., Vogs, A., & Strigul, N. S. (2015). 3D tree dimensionality assessment using photogrammetry and small unmanned aerial vehicles. *PLoS ONE*, *10*(9), 1–21. https://doi.org/10.1371/journal.pone.0137765
Gbenga Ajayi, O., Anthony Salubi, A., Fredrick Angbas, A., & Godfrey Odigure, M. (2017). Generation of accurate digital elevation models from UAV acquired low percentage overlapping images. *International Journal of Remote SensingOnline) Journal International Journal of Remote Sensing*, *38*, 143–1161. https://doi.org/10.1080/01431161.2017.1285085
Gibbs, H. K., Brown, S., Niles, J. O., & Foley, J. A. (2007). Monitoring and estimating tropical forest carbon stocks: making REDD a reality. *Environ. Res. Lett*, *2*, 45023–13. https://doi.org/10.1088/1748-9326/2/4/045023
Gizachew, B., & Duguma, A. L. (2016). Forest Carbon Monitoring and Reporting for REDD+: What Future for Africa? *Environmental Management*, *58*, 922–930. https://doi.org/10.1007/s00267-016-0762-7
Goetz, S. J., Hansen, M., Houghton, R. A., Walker, W., Laporte, N., & Busch, J. (2015). Measurement and monitoring needs, capabilities and potential for addressing reduced emissions from deforestation and forest degradation under REDD+. *Environmental Research Letters*, *10*(12), 123001. https://doi.org/10.1088/1748-9326/10/12/123001
Gougeon, F. A. (1995). A Crown-Following Approach to the Automatic Delineation of Individual Tree Crowns in High Spatial Resolution Aerial Images. *Canadian Journal of Remote Sensing*, *21*(3), 274–284. Retrieved from http://www.cfs.nrcan.gc.ca/pubwarehouse/pdfs/4583.pdf
Grace, J., Mitchard, E., & Gloor, E. (2014). Perturbations in the carbon budget of the tropics. *Global Change Biology*, *20*(10), 3238–3255. https://doi.org/10.1111/gcb.12600
Gschwantner, T., Schadauer, K., Vidal, C., Lanz, A., Tomppo, E., di Cosmo, L., … Duursma, E. (2009).

Common Tree Definitions for National Forest Inventories in Europe. *Silva Fennica*, *43*(2). Retrieved from http://www.metla.fi/silvafennica/full/sf43/sf432303.pdf
Harvey, M. C., Rowland, J. V., & Luketina, K. M. (2016). Drone with thermal infrared camera provides high resolution georeferenced imagery of the Waikite geothermal area, New Zealand. *Journal of Volcanology and Geothermal Research*, *325*, 61–69. https://doi.org/10.1016/j.jvolgeores.2016.06.014
Hemery, G. E., Savill, P. S., & Pryor, S. N. (2005). Applications of the crown diameter-stem diameter relationship for different species of broadleaved trees. *Forest Ecology and Management*, *215*(1–3), 285–294. https://doi.org/10.1016/j.foreco.2005.05.016
Houghton, R. A., House, J. I., Pongratz, J., Van Der Werf, G. R., Defries, R. S., Hansen, M. C., … Ramankutty, N. (2012). Carbon emissions from land use and land-cover change. *Biogeosciences*, *9*, 5125–5142. https://doi.org/10.5194/bg-9-5125-2012
Huang, S., Hager, S. a, Halligan, K. Q., Fairweather, I. S., Swanson, a K., & Crabtree, R. L. (2009). A comparison of individual tree and forest plot height derived from lidar and InSAR. *Photogrammetric Engineering and Remote Sensing*, *75*(2), 159–167. https://doi.org/10.14358/PERS.75.2.159
Hunter, M. O., Keller, M., Victoria, D., & Morton, D. C. (2013). Tree height and tropical forest biomass estimation. *Biogeosciences*, *10*(12), 8385–8399. https://doi.org/10.5194/bg-10-8385-2013
Hyyppä, H., Yu, X., Hyyppä, J., Kaartinen, H., Kaasalainen, S., Honkavaara, E., & Rönnholm, P. (2005). Factors affecting the quality of DTM generation in forested areas. In *Remote Sensing and …* (pp. 85–90). https://doi.org/10.3390/s120506347
Hyyppä, J., Hyyppä, H., Leckie, D., Gougeon, F., Yu, X., & Maltamo, M. (2008). Review of methods of small footprint airborne laser scanning for extracting forest inventory data in boreal forests. *International Journal of Remote Sensing*, *29*(5), 1339–1366. https://doi.org/10.1080/01431160701736489
Kankare, V., Holopainen, M., Vastaranta, M., Puttonen, E., Yu, X., Hyyppä, J., … Alho, P. (2013). Individual tree biomass estimation using terrestrial laser scanning. *ISPRS Journal of Photogrammetry and Remote Sensing*, *75*, 64–75. https://doi.org/10.1016/j.isprsjprs.2012.10.003
Karna, Y. K., Hussin, Y. A., Gilani, H., Bronsveld, M. C., Murthy, M. S. R., Qamer, F. M., … Baniya, C. B. (2015). Integration of WorldView-2 and airborne LiDAR data for tree species level carbon stock mapping in Kayar Khola watershed, Nepal. *International Journal of Applied Earth Observation and Geoinformation*, *38*, 280–291. https://doi.org/10.1016/j.jag.2015.01.011
Kenzo, T., Furutani, R., Hattori, D., Kendawang, J. J., Tanaka, S., Sakurai, K., & Ninomiya, I. (2009). Allometric equations for accurate estimation of above-ground biomass in logged-over tropical rainforests in Sarawak, Malaysia. *Journal of Forest Research*, *14*(6), 365–372. https://doi.org/10.1007/s10310-009-0149-1
Khatry Chhetri, D. B., & Fowler, G. W. (1996). Prediction models for estimating total heights of trees from diameter at breast height measurements in Nepal's lower temperate broad-leaved forests. *Forest Ecology and Management*, *84*(1–3), 177–186. https://doi.org/10.1016/0378-1127(96)03726-7
Kim, J. Y., Im, R.-Y., Do, Y., Kim, G.-Y., & Joo, G.-J. (2016). Above-ground biomass estimation of tuberous bulrush (Bolboschoenus planiculmis) in mudflats using remotely sensed multispectral image. *Ocean Science Journal*, *51*(1), 151–158. https://doi.org/10.1007/s12601-016-0013-0
Kumar Shah, S. (2011). *Modelling the Relationship Between Tree Canopy Projection Area and Above Ground Carbon Stock Using High Resolution Geoeye Satellite Images*. Unpublished Masters Thesis, University of Twente, Enschede, The Netherlands. Retrieved from http://www.itc.nl/library/papers_2011/msc/nrm/shah.pdf
Lim, Ye Seul La, Phu Hien Park, Jong Soo Lee, M. H., & Pyeon, Mu Wook Kim, J.-I. (2015). Calculation of Tree Height and Canopy Crown from Drone Images Using Segmentation. *Journal of the Korean Society of Surveying, Geodesy, Photogrammetry and Cartography*, *33*(6), 605–613. https://doi.org/DOI : 10.7848/ksgpc.2015.33.6.605
Lisein, J., Pierrot-Deseilligny, M., Bonnet, S., & Lejeune, P. (2013). A photogrammetric workflow for the creation of a forest canopy height model from small unmanned aerial system imagery. *Forests*, *4*(4), 922–944. https://doi.org/10.3390/f4040922
Malhi, Y. (2010). The carbon balance of tropical forest regions, 1990–2005. *Current Opinion in Environmental Sustainability*, *2*(4), 237–244. https://doi.org/10.1016/j.cosust.2010.08.002
Mauya, E., Hansen, E., Gobakken, T., Bollandsås, O., Malimbwi, R., & Næsset, E. (2015). Effects of field plot size on prediction accuracy of aboveground biomass in airborne laser scanning-assisted inventories in tropical rain forests of Tanzania. *Carbon Balance and Management*, *10*(1), 10. https://doi.org/10.1186/s13021-015-0021-x
Mbaabu, P. R., Hussin, Y. A., Weir, M., & Gilani, H. (2014). Quantification of carbon stock to understand

two different forest management regimes in Kayar Khola watershed, Chitwan, Nepal. *Journal of the Indian Society of Remote Sensing*, *42*(4), 745–754. https://doi.org/10.1007/s12524-014-0379-3

Mesner, N., & Oštir, K. (2014). Investigating the impact of spatial and spectral resolution of satellite images on segmentation quality. *Journal of Applied Remote Sensing*, *8*(1), 83696. https://doi.org/10.1117/1.JRS.8.083696

Möller, M., Lymburner, L., & Volk, M. (2009). The comparison index: A tool for assessing the accuracy of image segmentation. *International Journal of Applied Earth Observation and Geoinformation*, *9*(2007), 311–321. https://doi.org/10.1016/j.jag.2006.10.002

Molto, Q., Rossi, V., & Blanc, L. (2013). Error propagation in biomass estimation in tropical forests. *Methods in Ecology and Evolution*, *4*(2), 175–183. https://doi.org/10.1111/j.2041-210x.2012.00266.x

Morel, A. C., Saatchi, S. S., Malhi, Y., Berry, N. J., Banin, L., Burslem, D., … Ong, R. C. (2011). Estimating aboveground biomass in forest and oil palm plantation in Sabah, Malaysian Borneo using ALOS PALSAR data. *Forest Ecology and Management*, *262*(9), 1786–1798. https://doi.org/10.1016/j.foreco.2011.07.008

Moskal, L. M., & Zheng, G. (2011). Retrieving Forest Inventory Variables with Terrestrial Laser Scanning (TLS) in Urban Heterogeneous Forest. *Remote Sensing*, *4*(12), 1–20. https://doi.org/10.3390/rs4010001

Mtui, Y. P. (2017). *Tropical rainforest above Ground Biomass and Carbon Stock Estimation for Upper and Lower canopies Using Terrestrial Laser Scanner and Canopy Height Model from Unmanned Aerial Vehicle (UAV) in Ayer-Hitam, Malaysia*. Unpublished Masters Thesis, University of Twente, Enschede, The Netherlands. Retrieved from http://www.itc.nl/library/papers_2017/msc/nrm/mtui.pdf

Næsset, E., & Økland, T. (2002). Estimating tree height and tree crown properties using airborne scanning laser in a boreal nature reserve. *Remote Sensing of Environment*, *79*(1), 105–115. https://doi.org/10.1016/S0034-4257(01)00243-7

Nie, S., Wang, C., Zeng, H., Xi, X., & Li, G. (2017). Above-ground biomass estimation using airborne discrete-return and full-waveform LiDAR data in a coniferous forest. *Ecological Indicators*, *78*, 221–228. https://doi.org/10.1016/j.ecolind.2017.02.045

Okojie, J. A. (2017). *Assessment of Forest Tree Structural Parameter Extractability From Optical Imaging Uav Datasets, in Ahaus Germany*. Unpublished Masters Thesis, University of Twente, Enschede, The Netherlands. https://doi.org/10.13140/RG.2.2.29630.28484

Petrokofsky, G., Kanamaru, H., Achard, F., Goetz, S. J., Joosten, H., Holmgren, P., … Wattenbach, M. (2012). Comparison of methods for measuring and assessing carbon stocks and carbon stock changes in terrestrial carbon pools. How do the accuracy and precision of current methods compare? A systematic review protocol. *Environmental Evidence*, *1*(1), 6. https://doi.org/10.1186/2047-2382-1-6

Pix4D. (2017). Menu Process > Processing Options... > 1. Initial Processing > Calibration – Support. Retrieved December 14, 2017, from https://support.pix4d.com/hc/en-us/articles/205327965#gsc.tab=0

Puliti, S., Olerka, H., Gobakken, T., & Næsset, E. (2015). Inventory of Small Forest Areas Using an Unmanned Aerial System. *Remote Sensing*, *7*(8), 9632–9654. https://doi.org/10.3390/rs70809632

Rajpar, M. N., & Zakaria, M. (2014). Assessing the effects of logging activities on avian richness and diversity in different aged post-harvested hill dipterocarp tropical rainforest of Malaysia. *American Journal of Applied Sciences*, *11*(9), 1519–1529. https://doi.org/10.3844/ajassp.2014.1519.1529

Reuben, J. (2017). *Accuracy of Tree Height Derived from Point Clouds of of UAV Compared to Airborne LiDAR and Its Effect on Estimating Biomass and Carbon Stock in Part of Tropical Forest in Malaysia(Master's Thesis).* Unpublished Masters Thesis, University of Twente, Enschede, The Netherlands. Retrieved from https://ezproxy.utwente.nl:2315/library/2017/msc/nrm/hongoa.pdf

Reutebuch, S. E., Mcgaughey, R. J., Andersen, H.-E., & Carson, W. W. (2003). Accuracy of a high-resolution lidar terrain model under a conifer forest canopy. *Can. J. Remote Sensing*, *29*(5), 527–535. Retrieved from http://www.tandfonline.com/doi/pdf/10.5589/m03-022?needAccess=true

Ritchie, J. C. (1996). Remote sensing applications to hydrology: airborne laser altimeters. *Hydrological Sciences Journal*, *41*(4), 625–636. https://doi.org/10.1080/02626669609491529

Rodríguez-Veiga, P., Wheeler, J., Louis, V., Tansey, K., & Balzter, H. (2017). Quantifying Forest Biomass Carbon Stocks From Space. *Current Forestry Reports*, 1–18. https://doi.org/10.1007/s40725-017-0052-5

Ruiz, L. A., Hermosilla, T., Mauro, F., & Godino, M. (2014). Analysis of the influence of plot size and LiDAR density on forest structure attribute estimates. *Forests*, *5*(5), 936–951.

https://doi.org/10.3390/f5050936
Salleh, M. R. M., Ismail, Z., & Rahman, M. Z. A. (2015). Accuracy Assessment of Lidar-Derived Digital Terrain Model (Dtm) With Different Slope and Canopy Cover in Tropical Forest Region. *ISPRS Annals of Photogrammetry, Remote Sensing and Spatial Information Sciences*, *II-2/W2*(October), 183–189. https://doi.org/10.5194/isprsannals-II-2-W2-183-2015
Shahbazi, M., Théau, J., & Ménard, P. (2017). GIScience & Remote Sensing Recent applications of unmanned aerial imagery in natural resource management Recent applications of unmanned aerial imagery in natural resource management. https://doi.org/10.1080/15481603.2014.926650
Shimano, K. (1997). Analysis of the Relationship between DBH and Crown Projection Area Using a New Model. *J. For. Res*, *2*, 237–242. Retrieved from https://link.springer.com/content/pdf/10.1007%2FBF02348322.pdf
Simpson, J. E., Smith, T. E. L., & Wooster, M. J. (2017). Assessment of errors caused by forest vegetation structure in airborne LiDAR-derived DTMs. *Remote Sensing*, *9*(11). https://doi.org/10.3390/rs9111101
Suzuki, R., Kim, Y., & Ishii, R. (2013). Sensitivity of the backscatter intensity of ALOS/PALSAR to the above-ground biomass and other biophysical parameters of boreal forest in Alaska. https://doi.org/10.1016/j.polar.2013.03.001
Tang, L., & Shao, G. (2015). Drone remote sensing for forestry research and practices. *Journal of Forestry Research*, *26*(4), 791–797. https://doi.org/10.1007/s11676-015-0088-y
Tao, S., Guo, Q., Li, L., Xue, B., Kelly, M., Li, W., … Su, Y. (2014). Airborne Lidar-derived volume metrics for aboveground biomass estimation: A comparative assessment for conifer stands. *Agricultural and Forest Meteorology*, *198–199*, 24–32. https://doi.org/10.1016/j.agrformet.2014.07.008
Thiel, C., & Schmullius, C. (2017). Comparison of UAV photograph-based and airborne lidar-based point clouds over forest from a forestry application perspective. *International Journal of Remote SensingOnline) Journal International Journal of Remote Sensing*, *38*, 143–1161. https://doi.org/10.1080/01431161.2016.1225181
Tomaštík, J., Mokroš, M., Saloš, S., Chudỳ, F., & Tunák, D. (2017). Accuracy of photogrammetric UAV-based point clouds under conditions of partially-open forest canopy. *Forests*, *8*(5). https://doi.org/10.3390/f8050151
Tsui, O. W., Coops, N. C., Wulder, M. A., Marshall, P. L., & Mccardle, A. (2012). Using multi-frequency radar and discrete-return LiDAR measurements to estimate above-ground biomass and biomass components in a coastal temperate forest. https://doi.org/10.1016/j.isprsjprs.2012.02.009
van Leeuwen, M., & Nieuwenhuis, M. (2010). Retrieval of forest structural parameters using LiDAR remote sensing. *European Journal of Forest Research*, *129*(4), 749–770. https://doi.org/10.1007/s10342-010-0381-4
Vastaranta, M., Wulder, M. A., White, J. C., Pekkarinen, A., Tuominen, S., Ginzler, C., … Hyyppä, H. (2013). Airborne laser scanning and digital stereo imagery measures of forest structure: comparative results and implications to forest mapping and inventory update. *Canadian Journal of Remote Sensing*, *39*(5), 382–395. https://doi.org/10.5589/m13-046
Wallace, L., Lucieer, A., Malenovsk, Z., Turner, D., & Petr, V. (2016). Assessment of forest structure using two UAV techniques: A comparison of airborne laser scanning and structure from motion (SfM) point clouds. *Forests*, *7*(3), 1–16. https://doi.org/10.3390/f7030062
Zaki, N. A. M., Latif, Z. A., Suratman, M. N., & Zainal, M. Z. (2016). Modelling the Carbon Stocks Estimation of the Tropical Lowland Dipterocarp Forest Using Lidar and Remotely Sensed Data. *B Applied Remote Sensing & Geospatial Research Group*, *III*(July), 12–19. https://doi.org/10.5194/isprsannals-III-7-187-2016
Zarco-Tejada, P. J., Diaz-Varela, R., Angileri, V., & Loudjani, P. (2014). Tree height quantification using very high resolution imagery acquired from an unmanned aerial vehicle (UAV) and automatic 3D photo-reconstruction methods. *European Journal of Agronomy*, *55*, 89–99. https://doi.org/10.1016/j.eja.2014.01.004
Zhan, Q., Molenaar, M., Tempfli, K., & Shi, W. (2007). Quality assessment for geo-spatial objects derived from remotely sensed data. *International Journal of Remote Sensing*, *26*(14), 2953–2974. https://doi.org/10.1080/01431160500057764

APPENDICES

Appendix 1: Data collection sheet

DATA COLLECTION SHEET, BERKELAH FOREST RESERVE, MALAYSIA.									
Author:			**Plot radius:**		**Slope: (%)**		**Date:**		
Plot centre		**Latitude:**			**Longitude:**		**Plot No:**		
ID	Tree No:	Latitude	Longitude	Species	DBH (cm)	Stem height	Tree shapes	Crown diam. (m)	Canopy density (%)

Appendix 2: Screenshot of the Airborne Lidar CHM and the area of overlap with the UAV CHM.